

Theory of the anomalous Hall effect from the Kubo formula and the Dirac equation

A. Crépieux* and P. Bruno

Max-Planck-Institut für Mikrostrukturphysik, Weinberg 2, 06120 Halle, Germany

(Received 24 January 2001; published 13 June 2001)

A model to treat the anomalous Hall effect is developed. Based on the Kubo formalism and on the Dirac equation, this model allows the simultaneous calculation of the skew-scattering and side-jump contributions to the anomalous Hall conductivity. The continuity and the consistency with the weak-relativistic limit described by the Pauli Hamiltonian is shown. For both approaches, Dirac and Pauli, the Feynman diagrams, which lead to the skew-scattering and the side-jump contributions, are underlined. In order to illustrate this method, we apply it to a particular case: a ferromagnetic bulk compound in the limit of weak-scattering and free-electrons approximation. Explicit expressions for the anomalous Hall conductivity for both skew-scattering and side-jump mechanisms are obtained. Within this model, the recently predicted “spin Hall effect” appears naturally.

DOI: 10.1103/PhysRevB.64.014416

PACS number(s): 72.15.Gd, 72.25.Ba, 72.10.Bg

I. INTRODUCTION

The Hall resistivity of magnetic materials, in addition to the normal part proportional to the magnetic field, contains a supplementary part proportional to the magnetization, called the anomalous Hall resistivity

$$\rho_H = R_0 H + R_S M, \quad (1)$$

where R_0 and R_S are the normal and anomalous Hall coefficients, respectively, H the magnetic field, and M the magnetization. While the normal Hall effect results from the Lorenz force, the anomalous Hall effect is due to the spin-orbit coupling in the presence of spin polarization. Experimentally, the normal and anomalous parts can be extracted by measuring the Hall resistivity as a function of the magnetic field. At high magnetic field, when the magnetic saturation is reached, we get a linear variation of the Hall resistivity with a slope related to R_0 and an extrapolated value at zero magnetic field related to R_S . The normal and anomalous Hall coefficients have been determined for a large number of bulk alloys. These studies¹⁻⁵ reveal that the sign of R_S can change according to the alloy composition and that $|R_S M|$ is generally larger than $|R_0 H|$ for typical values of the magnetic field.

For different reasons, renewed attention to the anomalous Hall effect is observed quite recently. It is not only due to the increasing interest in spin-dependent transport phenomena but also because of some particular and interesting behaviors of the anomalous Hall resistivity obtained experimentally in granular alloys,⁶ in magnetic films,⁷ and multilayers.⁸ In addition, the anomalous Hall effect is increasingly used as a measurement tool to detect, for example, magnetization,⁹ dynamics of magnetic domains,¹⁰ or perpendicular anisotropy.¹¹ In addition, a new effect closely related to the anomalous Hall effect, the “spin Hall effect,” has recently been predicted.¹²

In the 1960's, a number of theoretical works¹³⁻¹⁶ attempted to elucidate the physical mechanisms responsible for the anomalous Hall effect and to calculate an explicit expression for the anomalous Hall resistivity. A series of controversies¹⁷⁻¹⁹ arose from those pioneering works which

were solved through detailed calculations²⁰ and comparisons.²¹ It is now accepted²² that two mechanisms are responsible for the anomalous Hall effect: the skew-scattering proposed by Smit¹⁴ and the side-jump proposed by Berger.¹⁶

An illustrative picture of these mechanisms is given in Fig. 1. Consider an incident plane wave characterized by a wave vector \mathbf{k} which is scattered by a central potential due, for example, to impurity. In the presence of spin-orbit coupling, the amplitude of the wave packet becomes anisotropic in the sense that it depends of the relative directions of the scattered and incident waves and of the spin. After a succession of scattering events, the average trajectory of the electron is deflected by a spin-dependent angle, which is typically of order 10^{-2} rad. This first mechanism, depicted by diagram (a) in Fig. 1, corresponds to the skew-scattering. The second mechanism corresponds to a lateral displacement, $\delta \approx 10^{-11}$ m, of the center of the wave-packet during the scattering, which is also spin dependent. This mechanism, depicted by diagram (b) in Fig. 1, corresponds to the side jump. In both cases, due to the spin-orbit coupling, the effect is asymmetrical in respect to the spin state. The spin-up and spin-down currents are then different. In magnetic materials, this leads to a nonzero spin current and to a transverse component in the charge current, which corresponds to the anomalous Hall effect.

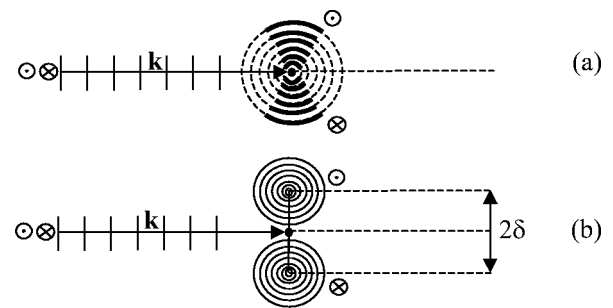


FIG. 1. Schematic picture of the skew-scattering (a) and side-jump (b) mechanisms from a quantum point of view (\odot corresponds to spin up and \otimes to spin down). The bold curves represent the anisotropic enhancement of the amplitude of the wave-packet due to spin-orbit coupling.

The skew scattering and the side-jump mechanisms give different contributions to the anomalous Hall resistivity. For bulk material, it has been shown that, in certain limits, the skew-scattering contribution is simply proportional to the resistivity^{14,15} while the side-jump contribution is proportional to the square of the resistivity.¹⁶ Then, we should have the simple expression

$$\tilde{\rho}_H = \tilde{\rho}_{yx} = a\tilde{\rho}_{xx} + b\tilde{\rho}_{xx}^2, \quad (2)$$

which implies that the relative importance of these two contributions depends both on the temperature and on the impurity concentration. However, we show in this paper that, even if the relation (2) remains correct, the skew-scattering mechanism contributes also to the quadratic term in the case of impurity scattering. Such behavior has already been shown by Kondorskii *et al.*²³

The traditional way to calculate the anomalous Hall resistivity is to include the contribution of spin-orbit coupling in the transition probability (it leads to the skew-scattering provided one goes beyond the Born approximation) and in the velocity (it leads to the so-called anomalous velocity which gives the side jump). While the skew scattering can be obtained in a classical approach it is claimed that the side jump is a pure quantum effect. We shall discuss this point in the Sec. II of this paper. Most of the calculations of the anomalous Hall resistivity are based on the Boltzmann equation and used severe approximations, in particular concerning the side-jump contribution. Some calculations²³ are based on the Kubo formalism, but surprisingly it is claimed that the side-jump contribution vanishes, and only the skew-scattering contribution is calculated.

Although the anomalous Hall effect is an old phenomena which has motivated a lot of experimental and theoretical studies, a unified model, able to calculate the skew-scattering and side-jump contributions on the same footing, was still missing. In this paper, we propose such a model. It is based on the Kubo formalism and has the peculiarity to be built from the Dirac equation. The justification for such an approach is given in Sec. III where we discuss in detail two different approaches for solving the anomalous Hall effect, i.e., based on Dirac and Pauli equations, and study the consistency in the weak-relativistic limit of the expressions of the conductivity tensors obtained in these two approaches. In Sec. IV, we calculate the anomalous Hall conductivity of a disordered ferromagnetic bulk compound. The results are discussed in Sec. V.

II. COMMENTS ON THE PHYSICAL NATURE OF THE SIDE-JUMP MECHANISM

It is often believed that the side-jump is a pure quantum effect and has no classical equivalent.²² The usual description of the side jump is then based on a quantum picture [see Fig. 1(b)] of a plane-wave transformed by scattering in the presence of spin-orbit coupling into a spherical wave whose center is shifted in a lateral direction (perpendicular to the momentum and to the spin). The sign of the displacement is opposite for spin up ($s=1$) and spin down ($s=-1$). A simple calculation in terms of phase-shift allows to deter-

mine this displacement. We start from the Pauli Hamiltonian

$$H = \frac{p^2}{2m} - \mu_B(\boldsymbol{\sigma} \cdot \mathbf{B}_{\text{eff}}) + W = H_0 + W, \quad (3)$$

where $\boldsymbol{\sigma}$ is the Pauli matrix, \mathbf{B}_{eff} the effective magnetic field due to exchange-correlation energy, and W the total potential including the spin-orbit coupling

$$W = V + \frac{\hbar}{4m^2c^2}(\boldsymbol{\sigma} \times \nabla V) \cdot \mathbf{p}. \quad (4)$$

The state of the system $|\Psi_{ks}\rangle$ after scattering is given in the Born approximation by the Lippmann-Schwinger equation $|\Psi_{ks}\rangle = |k, s\rangle + \sum_{k', s'} |k', s'\rangle G_0(\mathbf{k}', s', \varepsilon_k^s) \langle k', s' | W | k, s \rangle$, where ε_k^s and G_0 are, respectively, the eigenvalues and the Green's function associated with H_0 . The matrix elements of the potential are

$$\langle k', s' | W | k, s \rangle = \tilde{V}_{\mathbf{k}\mathbf{k}'} \left(\delta_{ss'} + \frac{i\hbar^2}{4m^2c^2} (\boldsymbol{\sigma}_{s's} \times \mathbf{k}') \cdot \mathbf{k} \right), \quad (5)$$

where $\tilde{V}_{\mathbf{k}\mathbf{k}'}$ is the Fourier transform of V . As the spin-orbit term is imaginary, it will influence the phase of the spherical wave. Thus, for small spin-orbit coupling, the wave function $\Psi_{ks}(\mathbf{r}) = \langle \mathbf{r} | \Psi_{ks} \rangle$ which describes the wave after scattering can be expressed as

$$\Psi_{ks}(\mathbf{r}) \propto e^{i\mathbf{r} \cdot \mathbf{k}} + \sum_{k', s'} \delta_{ss'} G_0(\mathbf{k}' s', \varepsilon_k^s) \tilde{V}_{\mathbf{k}\mathbf{k}'} e^{i\mathbf{r}'_s \cdot \mathbf{k}'}, \quad (6)$$

where we have assumed that the effective magnetic field is along the z direction. The center of the wave packet after scattering is given by

$$\mathbf{r}'_s \equiv \mathbf{r} + \frac{\hbar^2}{4m^2c^2} (\boldsymbol{\sigma}_{ss} \times \mathbf{k}), \quad (7)$$

which is clearly spin dependent and means that the shift of the center of the wave packet is different for spin up and spin down. The lateral displacement, defined as $\boldsymbol{\delta}^s \equiv \mathbf{r}'_s - \mathbf{r}$, is then equal to

$$\boldsymbol{\delta}^s = \frac{\lambda^2}{4\hbar} (\boldsymbol{\sigma}_{ss} \times \mathbf{p}), \quad (8)$$

where we have introduced the length λ which corresponds to the Compton wave length $\lambda_c = \hbar/mc$ in the case of free electrons. In real materials, Berger¹⁶ has shown that the spin-orbit coupling (i.e., λ^2) is renormalized by band structure effects by a factor $\alpha \approx 10^4$. We then obtain a lateral displacement $\boldsymbol{\delta}$ which is independent of disorder and of order $\lambda^2 k_F / 4 \approx \alpha \lambda_c^2 k_F / 4 \approx 10^{-11}$ m, in agreement with experimental results. Identical expression for $\boldsymbol{\delta}$ was originally derived by Lyo *et al.*²¹

In a pure classical picture, such a lateral displacement can be experienced by a particle with spin. As a simple example, consider an electron with a charge e ($e < 0$) subject to a uniform electric field $\mathbf{E} = E\mathbf{u}_x$ ($E > 0$) in the region $x > 0$; there is no field in the region $x < 0$. An incident electron

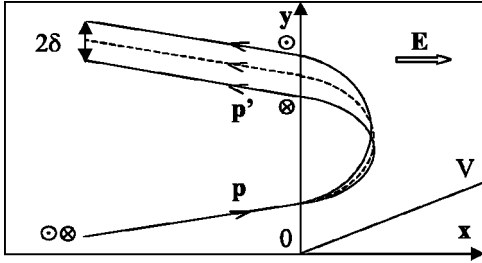


FIG. 2. Classical picture of the side-jump mechanism. The dashed line corresponds to the nonrelativistic trajectory of the particle and the solid lines to the relativistic trajectories for spin up (⊙) and spin down (⊗).

coming from the region $x < 0$ is reflected by the field as sketched in Fig. 2. The velocity is given by

$$\mathbf{v} = \frac{\partial H}{\partial \mathbf{p}} = \frac{\mathbf{p}}{m} - \frac{e\hbar}{4m^2c^2}(\boldsymbol{\sigma} \times \mathbf{E}), \quad (9)$$

and therefore contains an anomalous contribution $\mathbf{v}_a = -e\hbar(\boldsymbol{\sigma} \times \mathbf{E})/4m^2c^2$ arising from the spin-orbit interaction. In the field region ($x > 0$), where the trajectory is parabolic, the electron (we assume the spin to be along the z axis) has an anomalous velocity along the y axis, $v_a^y = -e\hbar(\sigma_z E)/4m^2c^2$. The electron therefore emerges with a shift along y , proportional to its spin σ_z . For an arbitrary electric field, the shift due to the anomalous velocity can be easily calculated

$$\delta = \int_{-\infty}^{+\infty} \mathbf{v}_a dt = - \int_{-\infty}^{+\infty} \frac{e\hbar}{4m^2c^2}(\boldsymbol{\sigma} \times \mathbf{E}) dt, \quad (10)$$

with $e\mathbf{E}dt = d\mathbf{p}$, so that

$$\delta = - \frac{\hbar \boldsymbol{\sigma}}{4m^2c^2} \times \int_{-\infty}^{+\infty} d\mathbf{p} = \frac{\lambda^2 \boldsymbol{\sigma}}{4\hbar} \times (\mathbf{p} - \mathbf{p}'). \quad (11)$$

In the above derivation, we have assumed that the spin is perpendicular to the scattering plane. The lateral displacement that we obtain is consistent with the one obtained in the quantum picture. Indeed, the parallel can be simply done by replacing in this classical calculation the momentum by a momentum operator and by making the angular average over the final momentum \mathbf{p}' : thus Eq. (11) coincides with Eq. (8).

III. COMPARISON OF THE DIRAC AND PAULI APPROACHES

Generally, the calculations of the anomalous Hall conductivity are based on the Pauli Hamiltonian. However, in our modelization, i.e., within the framework of the Kubo formalism, it appears to be simpler to adopt a relativistic approach based on the Dirac equation. To justify that, let us first remember the derivation of the skew scattering and the site-jump contributions in the Pauli approach. In presence of an exchange coupling, the Pauli Hamiltonian is $H = \tilde{H} + H_{rc}$ where \tilde{H} is the nonrelativistic Hamiltonian

$$\tilde{H} = \frac{p^2}{2m} - \mu_B(\boldsymbol{\sigma} \cdot \mathbf{B}_{\text{eff}}) + V, \quad (12)$$

and H_{rc} the first relativistic corrections to the Hamiltonian (order $1/c^2$)

$$H_{rc} = - \frac{p^4}{8m^3c^2} + \frac{\hbar}{4m^2c^2}(\boldsymbol{\sigma} \times \nabla V) \cdot \mathbf{p} + \frac{\hbar^2}{8m^2c^2}\Delta V + H_{\text{rxc}}, \quad (13)$$

which contains the relativistic mass correction, the spin-orbit coupling, the Darwin term and the relativistic correction to the exchange coupling H_{rxc} . Since the effect we are interested in results from the spin-orbit coupling, we do not need to give the explicit expression of H_{rxc} (calculations and comments on this term are presented in Ref. 31). In this work, we do not consider the contribution of the periodic part of the spin-orbit coupling (i.e., due to the lattice) but only the aperiodic part due to the presence of impurities. In the Pauli approach, the velocity contains two parts. One resulting from the nonrelativistic Hamiltonian $\tilde{\mathbf{v}} = \mathbf{p}/m$ and another one resulting from the relativistic corrections

$$\mathbf{v}_{rc} = - \frac{p^2 \mathbf{p}}{2m^3c^2} + \frac{\hbar}{4m^2c^2}(\boldsymbol{\sigma} \times \nabla V) + \mathbf{v}_{\text{rxc}}, \quad (14)$$

where \mathbf{v}_{rxc} is the velocity related to H_{rxc} . In this description, the spin-orbit contribution to the velocity [second term in Eq. (14)], the so-called anomalous velocity, appears in a natural and transparent way. When we insert this contribution in the Kubo formula, we obtain the side-jump contribution. It is also possible to isolate the spin-orbit contribution in the Green's function G associated with H by making the following expansion:

$$G = \tilde{G} + \tilde{G}H_{rc}\tilde{G} + \tilde{G}H_{rc}\tilde{G}H_{rc}\tilde{G} + \dots, \quad (15)$$

where \tilde{G} is the nonrelativistic Green's function associated with the nonrelativistic Hamiltonian \tilde{H} . When we insert this expression in the Kubo formula and proceed beyond the Born approximation, we obtain the skew-scattering contribution. Therefore, in the Pauli approach we get separately the skew-scattering and the side-jump contributions when the Green's functions and the velocities are respectively corrected by the spin-orbit coupling.

One important problem in the Pauli approach is to treat disorder. Actually, the spin-orbit coupling introduces two things: off-diagonal disorder (in the tight-binding approximation) and disorder in the velocity through the anomalous velocity. The second consequence is critical because it is then difficult to calculate precisely the vertex corrections and accordingly the anomalous Hall resistivity. To avoid these problems, we have chosen to base our model upon the Dirac equation instead of the Pauli equation. In presence of an exchange coupling, it has the form^{24,25}

$$H = c(\boldsymbol{\alpha} \cdot \mathbf{p}) + \beta mc^2 + V - \mu_B \beta(\boldsymbol{\sigma} \cdot \mathbf{B}_{\text{eff}}), \quad (16)$$

where the first term is the kinetic energy, the second term the mass energy, the third term is the potential, and the last one the exchange coupling. From Eq. (16), we see that the velocity is simply

$$\mathbf{v} = \frac{\partial H}{\partial \mathbf{p}} = c \boldsymbol{\alpha} = c \begin{pmatrix} 0 & \boldsymbol{\sigma} \\ \boldsymbol{\sigma} & 0 \end{pmatrix}. \quad (17)$$

At this level, there appears an apparent contradiction between the two approaches since, in the Dirac approach, contrary to the Pauli approach, we do not have any spin-orbit contribution to the velocity (anomalous velocity). It is therefore not clear *a priori* whether the side-jump mechanism would emerge from the Dirac approach. Actually, in the Dirac approach, the spin-orbit coupling, although it does not appear explicitly, is properly taken into account. Therefore, the conductivity should contain simultaneously the skew-scattering and side-jump contributions as well as higher order contributions in $1/c^2$. However, the expressions of the conductivity obtained in the Dirac and Pauli approaches should coincide in the weak-relativistic limit. To check this, we have calculated, in a formal manner, the weak-relativistic limit up to order $1/c^2$ of the conductivity obtained from the Dirac equation and compared it with the conductivity obtained from the Pauli equation. The determination of the conductivity tensor is performed in the Kubo formalism. In certain limits, the conductivity can be expressed as a product of operators, namely, Green's functions and velocities. However, the formulations proposed in the literature are often confused or even wrong^{26–28} concerning the off-diagonal el-

ements of the conductivity tensor due to an abusive generalization of the Kubo-Greenwood formula.²⁹ In order to clarify the situation, we present in Appendix A the derivation of the conductivity tensor from the original Kubo formula³⁵ and summarize the different stages and approximations which lead first to the Bastin formula³⁷ and finally to the Streda formula.³⁸ We show that the latter is a sum of two terms $\tilde{\sigma}_{ij}^I$ and $\tilde{\sigma}_{ij}^{II}$, respectively, given, in the limits of independent electrons approximation, zero temperature and zero frequency, by Eqs. (A14) and (A15):

$$\begin{aligned} \tilde{\sigma}_{ij} &= \tilde{\sigma}_{ij}^I + \tilde{\sigma}_{ij}^{II}, \\ \tilde{\sigma}_{ij}^I &\equiv \frac{e^2 \hbar}{4 \pi \Omega} \text{Tr} \langle v_i (G^+ - G^-) v_j G^- - v_i G^+ v_j (G^+ - G^-) \rangle_c, \\ \tilde{\sigma}_{ij}^{II} &\equiv - \frac{e^2}{4 i \pi \Omega} \text{Tr} \langle (G^+ - G^-) (r_i v_j - r_j v_i) \rangle_c, \end{aligned} \quad (18)$$

where i and j are the direction indices, Ω the volume of the sample, $\langle \dots \rangle_c$ denotes the configurational average, and G^+ and G^- are the retarded and advanced Green's functions at the Fermi level $G^\pm = G(\varepsilon_F \pm i0) = (\varepsilon_F \pm i0 - H)^{-1}$. The procedure that we follow is first to insert the Dirac velocity and Dirac Green's function in Eq. (18), next to perform a weak-relativistic expansion of $\tilde{\sigma}_{ij}$ and finally to compare it with the expression obtained in the Pauli approach. The Dirac velocity is given by Eq. (17) and for the Dirac Green's function, we have used an exact expression derived from Eq. (16) and given in Ref. 31 by Eq. (A3)

$$G^\pm = \begin{pmatrix} \tilde{G}^\pm - \tilde{G}^\pm \frac{\boldsymbol{\sigma} \cdot \mathbf{p}}{2mc} [\varepsilon_F - V - \mu_B (\boldsymbol{\sigma} \cdot \mathbf{B}_{\text{eff}})] D^\pm \frac{\boldsymbol{\sigma} \cdot \mathbf{p}}{2mc} \tilde{G}^\pm & \tilde{G}^\pm \frac{\boldsymbol{\sigma} \cdot \mathbf{p}}{2mc} (Q^\pm)^{-1} D^\pm Q^\pm \\ D^\pm \frac{\boldsymbol{\sigma} \cdot \mathbf{p}}{2mc} \tilde{G}^\pm & \frac{1}{2mc^2} D^\pm Q^\pm \end{pmatrix}, \quad (19)$$

where the operators D^\pm and Q^\pm are given by

$$D^\pm = \left(1 + Q^\pm \frac{[\varepsilon_F - V - \mu_B (\boldsymbol{\sigma} \cdot \mathbf{B}_{\text{eff}})]}{2mc^2} \right)^{-1}, \quad (20)$$

$$Q^\pm = 1 + \frac{(\boldsymbol{\sigma} \cdot \mathbf{p}) \tilde{G}^\pm (\boldsymbol{\sigma} \cdot \mathbf{p})}{2m}. \quad (21)$$

The details of the calculations are presented in Appendix B. The determination of the conductivity is done up to order $1/c^2$. It is shown that the identification with the Pauli approach is successful only when one considers the total conductivity $\tilde{\sigma}_{ij} = \tilde{\sigma}_{ij}^I + \tilde{\sigma}_{ij}^{II}$. Indeed, when we compare the expression of $\tilde{\sigma}_{ij}^I$ obtained in the Dirac approach [see Eq. (B5) for order $1/c^0$ and Eq. (B9) for order $1/c^2$] to the one obtained in Pauli approach, we obtained different terms which

are exactly canceled by terms in $\tilde{\sigma}_{ij}^{II}$ [see Eq. (B6) for order $1/c^0$ and Eq. (B10) for order $1/c^2$]. The nonrelativistic limit of the total conductivity obtained in the Dirac approach is

$$\begin{aligned} \tilde{\sigma}_{ij}^{(0)} &= \frac{e^2 \hbar}{4 \pi \Omega} \text{Tr} \left\langle \frac{p_i}{m} (\tilde{G}^+ - \tilde{G}^-) \frac{p_j}{m} \tilde{G}^- - \frac{p_i}{m} \tilde{G}^+ + \frac{p_j}{m} (\tilde{G}^+ - \tilde{G}^-) \right\rangle_c \\ &\quad - \frac{e^2}{4 i \pi \Omega} \text{Tr} \left\langle (\tilde{G}^+ - \tilde{G}^-) \left(r_i \frac{p_j}{m} - r_j \frac{p_i}{m} \right) \right\rangle_c, \end{aligned} \quad (22)$$

which corresponds exactly to the conductivity obtained from Eq. (18) when one inserts the nonrelativistic velocity $\tilde{\mathbf{v}} = \mathbf{p}/m$ and the nonrelativistic Green's function \tilde{G} . The last term in Eq. (22) is zero in absence of external magnetic field. The fact that a supplementary term in $\tilde{\sigma}_{ij}^{(0)}$ is present in the Dirac approach and not in the Pauli approach has serious consequences when one neglects $\tilde{\sigma}_{ij}^{II(0)}$ because it leads to an

additional contribution at order $1/c^0$ to the off-diagonal conductivity which does not disappear in the nonrelativistic limit and thus would give unphysical results. At order $1/c^2$, the total conductivity obtained in the Dirac approach is

$$\tilde{\sigma}_{ij}^{(2)} = \tilde{\sigma}_{ij}^{\text{SS}} + \tilde{\sigma}_{ij}^{\text{SJ}} + \tilde{\sigma}_{ij}^{\text{or}}, \quad (23)$$

where $\tilde{\sigma}_{ij}^{\text{SS}}$ contains the terms which lead to the skew scattering

$$\begin{aligned} \tilde{\sigma}_{ij}^{\text{SS}} = & \frac{e^2 \hbar}{4\pi\Omega} \text{Tr} \left\langle \frac{p_i}{m} (\tilde{G}^+ H_{rc} \tilde{G}^+ - \tilde{G}^- H_{rc} \tilde{G}^-) \frac{p_j}{m} \tilde{G}^- \right. \\ & + \frac{p_i}{m} (\tilde{G}^+ - \tilde{G}^-) \frac{p_j}{m} \tilde{G}^- H_{rc} \tilde{G}^- \\ & - \frac{p_i}{m} \tilde{G}^+ H_{rc} \tilde{G}^+ + \frac{p_j}{m} (\tilde{G}^+ - \tilde{G}^-) \\ & \left. - \frac{p_i}{m} \tilde{G}^+ + \frac{p_j}{m} (\tilde{G}^+ H_{rc} \tilde{G}^+ - \tilde{G}^- H_{rc} \tilde{G}^-) \right\rangle_c, \quad (24) \end{aligned}$$

$\tilde{\sigma}_{ij}^{\text{SJ}}$ contains the terms which lead to the side jump

$$\begin{aligned} \tilde{\sigma}_{ij}^{\text{SJ}} = & \frac{e^2 \hbar}{4\pi\Omega} \text{Tr} \left\langle (\mathbf{v}_{rc})_i (\tilde{G}^+ - \tilde{G}^-) \frac{p_j}{m} \tilde{G}^- \right. \\ & - (\mathbf{v}_{rc})_i \tilde{G}^+ + \frac{p_j}{m} (\tilde{G}^+ - \tilde{G}^-) \\ & + \frac{p_i}{m} (\tilde{G}^+ - \tilde{G}^-) (\mathbf{v}_{rc})_j \tilde{G}^- \\ & \left. - \frac{p_i}{m} \tilde{G}^+ + (\mathbf{v}_{rc})_j (\tilde{G}^+ - \tilde{G}^-) \right\rangle_c, \quad (25) \end{aligned}$$

and $\tilde{\sigma}_{ij}^{\text{or}}$ is equal to

$$\begin{aligned} \tilde{\sigma}_{ij}^{\text{or}} = & -\frac{e^2}{4i\pi\Omega} \text{Tr} \left\langle (\tilde{G}^+ - \tilde{G}^-) [r_i (\mathbf{v}_{rc})_j - r_j (\mathbf{v}_{rc})_i] \right. \\ & \left. + (\tilde{G}^+ H_{rc} \tilde{G}^+ - \tilde{G}^- H_{rc} \tilde{G}^-) \left(r_i \frac{p_j}{m} - r_j \frac{p_i}{m} \right) \right\rangle_c. \quad (26) \end{aligned}$$

In addition to the skew-scattering and side-jump contributions to the anomalous Hall effect, we identify a new contribution $\tilde{\sigma}_{ij}^{\text{or}}$ which is related to the orbital momentum $\mathbf{L} = \mathbf{r} \times \mathbf{p}$. The expression (23) of the conductivity corresponds exactly to the one which is obtained from Eq. (18) when one inserts the first order corrections to the velocity \mathbf{v}_{rc} and to the Green function $\tilde{G} H_{rc} \tilde{G}$ where \mathbf{v}_{rc} and H_{rc} are given, respectively, by Eqs. (13) and (14). We have then proved in the weak-relativistic limit (up to order $1/c^2$) the coincidence of the conductivity in the two approaches.

In summary, from the Pauli Hamiltonian, we get the skew-scattering and the side-jump contributions separately while, from the Dirac Hamiltonian, we get the both contributions and also higher order in $1/c^2$ contributions simulta-

neously. Therefore, in a full relativistic Dirac description, it will be difficult to assess the importance of each contributions. However, this approach has a great advantage over the Pauli approach: it allows a simpler treatment of the disorder because, in contrast to the Pauli approach where both the velocities and the Green's functions contain disorder, the disorder is only present in the Green's functions. It is thus possible to take one of the velocity operator outside of the configurational average and to calculate precisely the vertex corrections to the conductivity. For this reason, the Dirac approach should be more efficient to calculate the anomalous Hall resistivity.

In the next section, we present a direct application of our model. In order to perform the analytical calculations, we restrict ourselves to the weak-relativistic limit and to approximate calculations of the vertex corrections; then the results that we obtain can still be compared to the ones obtained from the Pauli approach.

IV. ANOMALOUS HALL CONDUCTIVITY OF A FERROMAGNETIC COMPOUND

In this section, we present the calculation of the anomalous Hall conductivity of a ferromagnetic bulk compound submitted to a potential. This calculation is done in both Dirac and Pauli approaches in order to show the similarities and the differences between these two approaches. We consider a system with a cubic symmetry and a magnetization along the z axis. Thus, the conductivity tensor has the form

$$\tilde{\sigma} = \begin{pmatrix} \tilde{\sigma}_{xx} & \tilde{\sigma}_{xy} & 0 \\ -\tilde{\sigma}_{xy} & \tilde{\sigma}_{xx} & 0 \\ 0 & 0 & \tilde{\sigma}_{zz} \end{pmatrix}. \quad (27)$$

We are only interested in the relativistic corrections to the off-diagonal elements which correspond to the anomalous Hall effect. We do not study the relativistic corrections to the diagonal elements which correspond to the anisotropic magnetoresistance (AMR) and lead to a difference of order $1/c^4$ between $\tilde{\sigma}_{xx}$ and $\tilde{\sigma}_{zz}$. Thus, in this work, the diagonal elements are calculated at order $1/c^0$ and by consequence are all equal, while the off-diagonal elements are calculated at order $1/c^2$. To get analytical expressions, we have made several approximations: free-electron approximation, weak-scattering limit and weak-relativistic limit for the Dirac approach. In Sec. III, we have shown that the conductivity is equal to

$$\begin{aligned} \tilde{\sigma}_{ij} = & \frac{e^2 \hbar}{4\pi\Omega} \text{Tr} \langle v_i (G^+ - G^-) v_j G^- - v_i G^+ v_j (G^+ - G^-) \rangle_c \\ & - \frac{e^2}{4i\pi\Omega} \text{Tr} \langle (G^+ - G^-) (r_i v_j - r_j v_i) \rangle_c, \quad (28) \end{aligned}$$

where the Green's function G^\pm is associated with the total Hamiltonian: $G^\pm = (\epsilon_F \pm i0 - H)^{-1} = (\epsilon_F \pm i0 - H_0 - W)^{-1}$ where H_0 is the nonperturbed Hamiltonian and W the perturbation (equal to the potential V in the Dirac approach and to $V + H_{\text{SO}}$ in the Pauli approach where H_{SO} is the spin-orbit

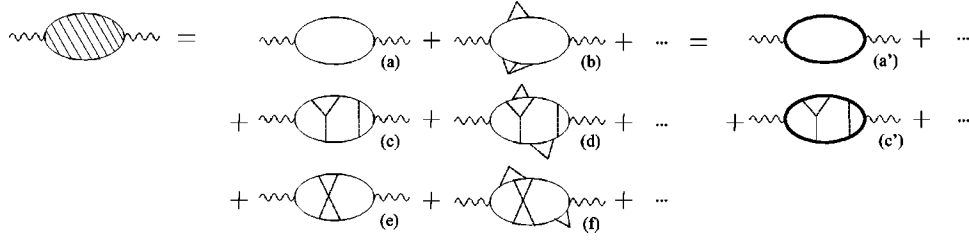


FIG. 3. Illustration of the conductivity with the help of Feynman diagrams. The total conductivity (hatched diagram), expressed as an infinite sum of diagrams involving the nondisordered Green's function G_0 (thin curve line), can be rewritten as an infinite sum of diagrams involving the average Green's function \underline{G} (bold curve line). The wave lines refer to the velocity and the dashed lines to the potential.

coupling). The explicit form of the potential V does not enter in the calculations, thus the results obtained below apply for both impurity scattering and phonon scattering in the adiabatic approximation. We modelize the compound in the following way: the total volume of the sample $\Omega = L^3$ is divided into N cells of volume $\Omega_0 = a^3$. In each cell, the potential takes a constant value V with a probability distribution $P(V)$ which is characterized by its moments $\langle V^n \rangle_c = \int P(V) V^n dV$. A proper choice of the energy origin yields $\langle V \rangle_c = 0$. We assume that there are no correlations in the value of the potential in different cells. In this first approach, we neglect in Eq. (28) the contribution of the terms which involves product of two advanced (or retarded) Green's functions. Such an approximation is justified in the weak-disorder limit.³² In Appendix B, we have shown that $\tilde{\sigma}_{ij}^{II}$, calculated in the Dirac approach, contains two parts, the first one related to the orbital momentum, which is negligible in our model, and the second one which is exactly compensated by terms in $\tilde{\sigma}_{ij}^I$. Then, we do not need to calculate this contribution. The conductivity reduces to

$$\tilde{\sigma}_{ij} = \frac{e^2 \hbar}{2\pi\Omega} \text{Tr} \langle v_i G^+ v_j G^- \rangle_c. \quad (29)$$

We introduce first the t matrix $T = W + WG_0 T$ which allows one to write the Green's function as $G = G_0 + G_0 T G_0$ where G_0 is the nonperturbed Green's function. Inserting this in Eq. (29), we get

$$\begin{aligned} \tilde{\sigma}_{ij} &= \frac{e^2 \hbar}{2\pi\Omega} \text{Tr} \langle v_i G_0^+ v_j G_0^- \rangle_c \\ &+ \frac{e^2 \hbar}{2\pi\Omega} \text{Tr} \langle v_i G_0^+ T G_0^+ v_j G_0^- T G_0^- \rangle_c. \end{aligned} \quad (30)$$

This equation can be illustrated with the help of Feynman diagrams as is done in Fig. 3. The conductivity $\tilde{\sigma}_{ij}$, represented by the full diagram, is then expressed as a sum of an infinite number of diagrams. Only few of them are depicted in Fig. 3: diagram (a) which corresponds to the first term in Eq. (30) and diagrams from (b)–(f) which are some representative samples of the kind of diagrams which give the second term in Eq. (30). The main approximation done in our calculation is to neglect the crossed diagrams which correspond to weak-localization corrections, i.e., we neglect diagrams such as (e) and (f) and we keep only the so-called

ladder diagrams. Weak-localization corrections to the anomalous Hall conductivity are discussed in a separate paper.³³ We introduce the configurational average Green's function $\underline{G} = \langle G \rangle_c$ which can be written with the help of the self-energy $\Sigma = \langle W G_0 W \rangle_c + \langle W G_0 W G_0 W \rangle_c + \dots$ since $\underline{G} = (\varepsilon_F - H_0 - \Sigma)^{-1}$. When we neglect the crossed diagrams, Eq. (30) can be written as

$$\begin{aligned} \tilde{\sigma}_{ij} &= \frac{e^2 \hbar}{2\pi\Omega} \text{Tr} \langle v_i \underline{G}^+ v_j \underline{G}^- \rangle_c \\ &+ \frac{e^2 \hbar}{2\pi\Omega} \text{Tr} \langle v_i \underline{G}^+ T' \underline{G}^+ v_j \underline{G}^- T' \underline{G}^- \rangle_c, \end{aligned} \quad (31)$$

with T' solution of $T' = W + W \underline{G} T'$. The first term in the right side hand is the so-called bubble term ($\equiv \tilde{\sigma}_{ij}^{\text{bubble}}$) and the second one corresponds to the vertex corrections ($\equiv \tilde{\sigma}_{ij}^{\text{vertex}}$). Within this transformation, the calculation of the conductivity is then reduced to two distinct problems: determination of the average Green's function (i.e., the self-energy) and calculation of the vertex corrections. Because of the weak-scattering limit, we keep in the self-energy and the t matrix the lowest sufficient orders

$$\begin{cases} \Sigma = \langle W G_0 W \rangle_c, \\ T' = W + W \underline{G} W. \end{cases} \quad (32)$$

In the t matrix, we have to keep the terms up to the second order with V because it is necessary to go beyond the Born approximation to get the skew scattering.¹⁴ The explicit calculation of Eq. (31) in the approximations (32) for the Dirac and Pauli approaches is presented in the next two sections.

A. Dirac approach

We assume free electrons in a uniform effective magnetic field \mathbf{B}_{eff} parallel to the z axis and submitted to a potential. The nonperturbed part of the Hamiltonian is

$$H_0 = c(\boldsymbol{\alpha} \cdot \mathbf{p}) + (\beta - 1) m c^2 - \mu_B \beta \sigma_z B_{\text{eff}}, \quad (33)$$

and the perturbation part is simply the potential $W = V$. The matrix elements of the average Green's function are $\langle k, s | \underline{G}^\pm | k, s \rangle = (\varepsilon_F - \varepsilon_k^\pm \pm i\hbar/2\tau_k^\pm)^{-1}$ where the eigenvalues ε_k^\pm of Eq. (33) are in the weak-relativistic limit equals to

$$\varepsilon_k^s = \frac{\hbar^2 k^2}{2m} - s\mu_B B_{\text{eff}} + o\left(\frac{1}{c^2}\right), \quad (34)$$

for the upper band, and

$$\varepsilon_{\underline{k}}^s = -2mc^2 + o\left(\frac{1}{c^0}\right), \quad (35)$$

for the lower band. The s index refers to the spin ($s=1$ for spin up and $s=-1$ for spin down), the k index refers to the upper band and the \underline{k} to the lower band. The lifetime τ_k^s which appears in the expression of the average Green's function is given by

$$\begin{aligned} \frac{\hbar}{2\tau_k^s} &= -\text{Im}\langle k, s | \Sigma^+ | k, s \rangle = -\text{Im}\langle k, s | \langle V G_0^+ V \rangle_c | k, s \rangle \\ &= \pi \Omega_0 \mathcal{N}_s(\varepsilon_k^s) \langle V^2 \rangle_c, \end{aligned} \quad (36)$$

where \mathcal{N}_s is the density of states of spin s by unit volume. In the Dirac approach, the velocity \mathbf{v} is simply equal to $c\boldsymbol{\alpha}$. Because we have chosen to work in the basis where the nonperturbed Hamiltonian H_0 (and by consequence the Green's function G_0) is diagonal, we have to calculate the velocity in this basis, we get

$$\mathbf{v} = \begin{pmatrix} \mathbf{u}(\mathbf{k}) + o\left(\frac{1}{c^2}\right), & c\boldsymbol{\sigma} + o\left(\frac{1}{c}\right) \\ c\boldsymbol{\sigma} + o\left(\frac{1}{c}\right), & o(c^0) \end{pmatrix}, \quad (37)$$

where $\mathbf{u}(\mathbf{k})$ is the (2×2) matrix

$$\mathbf{u}(\mathbf{k}) = \frac{\hbar \mathbf{k}}{m} \begin{pmatrix} 1 & 0 \\ 0 & 1 \end{pmatrix}. \quad (38)$$

We have now all the ingredients to calculate the bubble term in Eq. (31)

$$\begin{aligned} \tilde{\sigma}_{ij}^{\text{bubble}} &= \frac{e^2 \hbar}{2\pi\Omega} \sum_{kss'} \langle k, s | v_i | k, s' \rangle \langle k, s' | \underline{G}^+ | k, s' \rangle \\ &\quad \times \langle k, s' | v_j | k, s \rangle \langle k, s | \underline{G}^- | k, s \rangle. \end{aligned} \quad (39)$$

The configurational average $\langle \dots \rangle_c$ has been dropped because in the Dirac approach the velocity is a nondisordered quantity. At order $1/c^0$, only the diagonal elements ($s=s'$, no spin flip) of the velocity and the particles in the upper band contribute, then we have



FIG. 4. Bubble diagram contributing to the diagonal conductivity $\tilde{\sigma}_{xx}$. The signs $+/-$ refer to the retarded/advanced average Green's function \underline{G}^\pm .

$$\tilde{\sigma}_{ij}^{\text{bubble}} = \frac{e^2 \hbar^3}{2\pi m^2 \Omega} \sum_{ks} \frac{k_i k_j}{(\varepsilon_F - \varepsilon_k^s)^2 + \frac{\hbar^2}{4(\tau_k^s)^2}}. \quad (40)$$

The dispersion law ε_k^s given by Eq. (34) is isotropic at order $1/c^0$. Then, the angular dependence is entirely contained in the factor $k_i k_j$, which means that only diagonal components of the conductivity are different from zero. To order $1/c^0$, the vertex corrections to the diagonal components vanish, so that the total conductivity $\tilde{\sigma}_{ii}$ is equal to $\tilde{\sigma}_{ii}^{\text{bubble}}$. After integration over k , we get

$$\tilde{\sigma}_{xx} = e^2 \mathcal{N}_\uparrow \frac{l^\uparrow v_F^\uparrow}{3} + e^2 \mathcal{N}_\downarrow \frac{l^\downarrow v_F^\downarrow}{3} \equiv \tilde{\sigma}_{xx}^\uparrow + \tilde{\sigma}_{xx}^\downarrow, \quad (41)$$

which corresponds to the Einstein relation with two spin channels where $l^s = v_F^s \tau_F^s$ is the mean-free path, v_F^s and \mathcal{N}_s are the velocity and the density of states by unit volume at the Fermi energy for spin s , respectively (identical expressions are obtained for $\tilde{\sigma}_{yy}$ and $\tilde{\sigma}_{zz}$). The diagram which gives this contribution is depicted on Fig. 4.

The off-diagonal components of the conductivity arise only when we take the vertex corrections into account. If we expand the t matrix up to the second order in V , from Eq. (31), we get

$$\begin{aligned} \tilde{\sigma}_{ij}^{\text{vertex}} &= \frac{e^2 \hbar}{2\pi\Omega} \text{Tr} \langle v_i \underline{G}^+ (V + V \underline{G}^+ V) \underline{G}^+ \\ &\quad \times v_j \underline{G}^- (V + V \underline{G}^- V) \underline{G}^- \rangle_c. \end{aligned} \quad (42)$$

We then need the potential in the new basis

$$V = \tilde{V}(\mathbf{k}' - \mathbf{k}) \begin{pmatrix} U(\mathbf{k}, \mathbf{k}') + o\left(\frac{1}{c^4}\right), & \frac{\hbar(\boldsymbol{\sigma} \cdot \mathbf{k}')}{2mc} + o\left(\frac{1}{c^3}\right) \\ \frac{\hbar(\boldsymbol{\sigma} \cdot \mathbf{k}')}{2mc} + o\left(\frac{1}{c^3}\right), & o(c^0) \end{pmatrix}, \quad (43)$$

where $U(\mathbf{k}, \mathbf{k}')$ is the (2×2) matrix

$$U(\mathbf{k}, \mathbf{k}') = \begin{pmatrix} 1 - \frac{\hbar^2[(\mathbf{k}' - \mathbf{k})^2 + 2i(\mathbf{k}' \times \mathbf{k}) \cdot \mathbf{e}_z]}{8m^2c^2} & \frac{\hbar^2[(k'_x - ik'_y)k'_z - (k_x - ik_y)k_z - i(\mathbf{k}' \times \mathbf{k}) \cdot (\mathbf{e}_x - i\mathbf{e}_y)]}{4m^2c^2} \\ \frac{\hbar^2[(k'_x + ik'_y)k'_z - (k_x + ik_y)k_z - i(\mathbf{k}' \times \mathbf{k}) \cdot (\mathbf{e}_x + i\mathbf{e}_y)]}{4m^2c^2} & 1 - \frac{\hbar^2[(\mathbf{k}' - \mathbf{k})^2 - 2i(\mathbf{k}' \times \mathbf{k}) \cdot \mathbf{e}_z]}{8m^2c^2} \end{pmatrix}, \quad (44)$$

and $\tilde{V}(\mathbf{q}) = \int d\mathbf{r} e^{i\mathbf{q} \cdot \mathbf{r}} V(\mathbf{r}) / \Omega$ is the Fourier transform of the potential. When we study in detail all the diagrams included in Eq. (42), we see that only two kind of diagrams³⁴ contribute to the conductivity at order $1/c^2$. These diagrams are depicted on Figs. 5 and 6 (left column).

The first series of diagrams (see Fig. 5) involves velocities at order $1/c^0$, Green's functions at order $1/c^0$, which means that only particles in the upper band contribute, and potential twice at order $1/c^0$ and once at order $1/c^2$ which ensures a total order of $1/c^2$ for the conductivity. The diagrams of this first series correspond to the skew-scattering mechanism. The second series of diagrams (left column in Fig. 6) involves one velocity at order $1/c^0$ and one at order c , three Green's functions at order $1/c^0$ and one at order $1/c^2$, which means that we have a transition of particles between the upper and lower bands, and potential one time at order $1/c^0$ and one time at order $1/c$ which ensures a total order of $1/c^2$ for the conductivity. The diagrams of this second series correspond to the side-jump mechanism. In the following, we present the explicit calculation of the conductivity due to these two series. Let us start with the skew scattering. We present the calculation of the diagram (a) in Fig. 5, which gives

$$\begin{aligned} \tilde{\sigma}_{xy}^{(5a)} = & \frac{e^2 \hbar}{2\pi\Omega} \sum_{kk's} \langle \langle k, s | v_x | k, s \rangle^{(0)} \langle k, s | \underline{G}^+ | k, s \rangle^{(0)} \\ & \times \langle k, s | V | k', s \rangle^{(0)} \langle k', s | \underline{G}^+ | k', s \rangle^{(0)} \\ & \times \langle k', s | V | k'', s \rangle^{(0)} \langle k'', s | \underline{G}^+ | k'', s \rangle^{(0)} \\ & \times \langle k'', s | v_y | k'', s \rangle^{(0)} \langle k'', s | \underline{G}^- | k'', s \rangle^{(0)} \\ & \times \langle k'', s | V | k, s \rangle^{(2)} \langle k, s | \underline{G}^- | k, s \rangle^{(0)} \rangle_c. \end{aligned} \quad (45)$$

The number in bracket indicates the order with respect to $1/c$ of the matrix elements like in Fig. 5 when the order is different than zero. We remark that for a total order $1/c^2$ of the conductivity, the spin is conserved during the process (no spin-flip scattering). We insert in this expression, the matrix

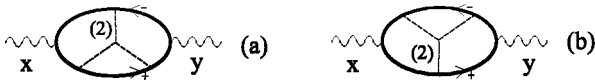


FIG. 5. Diagrams contributing to the off-diagonal conductivity $\tilde{\sigma}_{xy}$ through the skew-scattering mechanism in both Pauli and Dirac approaches. The number in bracket indicates the order with respect to $1/c$ of the matrix elements of the velocity (wave line), average Green's function (bold curve line), and potential (dashed line). It is omitted in case of zero order with $1/c$.

elements given by Eqs. (38) and (44) and perform the integration over k , k' , and k'' . The final contribution to the conductivity corresponding to the diagram (a) is a complex quantity. The calculation of the diagram (b) gives the conjugated expression, then the total contribution due to the skew-scattering mechanism is a real quantity equal to

$$\begin{aligned} \tilde{\sigma}_{xy}^{SS} = & -\frac{\pi m^2 \lambda^2}{6\hbar^2} \frac{\langle V^3 \rangle_c}{\langle V^2 \rangle_c} (\mathcal{N}_\uparrow \Omega_0 \tilde{\sigma}_{xx}^\uparrow (v_F^\uparrow)^2 - \mathcal{N}_\downarrow \Omega_0 \tilde{\sigma}_{xx}^\downarrow (v_F^\downarrow)^2) \\ \equiv & \tilde{\sigma}_{xy}^{SS\uparrow} + \tilde{\sigma}_{xy}^{SS\downarrow}. \end{aligned} \quad (46)$$

We turn now our attention to the side-jump mechanism. Diagram (a) of Fig. 6 gives

$$\begin{aligned} \tilde{\sigma}_{xy}^{(6a)} = & \frac{e^2 \hbar}{2\pi\Omega} \sum_{kk's} \langle \langle k, s | v_x | k, -s \rangle^{(-1)} \langle k, -s | \underline{G}^+ | k, -s \rangle^{(2)} \\ & \times \langle k, -s | V | k', s \rangle^{(1)} \langle k', s | \underline{G}^+ | k', s \rangle^{(0)} \\ & \times \langle k', s | v_y | k', s \rangle^{(0)} \langle k', s | \underline{G}^- | k', s \rangle^{(0)} \\ & \times \langle k', s | V | k, s \rangle^{(0)} \langle k, s | \underline{G}^- | k, s \rangle^{(0)} \rangle_c. \end{aligned} \quad (47)$$

In this mechanism, due to the presence of off-diagonal elements in the velocity (37) and the potential (43), a particle of

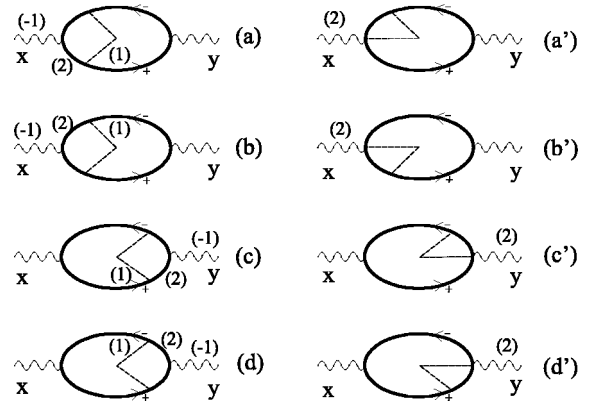


FIG. 6. Diagrams contributing to the off-diagonal conductivity $\tilde{\sigma}_{xy}$ through the side-jump mechanism in Dirac approach (left column) and Pauli approach (right column). The number in bracket indicates the order with respect to $1/c$ of the matrix elements of the velocity (wave line), average Green's function (bold curve line), and potential (dashed line).

the upper band ε_k^s experiences a virtual transition in the lower band ε_k^{-s} associated to the opposite spin. We perform the integrations over k and k' , add the contributions of Figs. 6(a)–6(d) and finally obtained

$$\tilde{\sigma}_{xy}^{SJ} = -e^2 \mathcal{N}_\uparrow \frac{2\delta^\uparrow v_F^\uparrow}{3} + e^2 \mathcal{N}_\downarrow \frac{2\delta^\downarrow v_F^\downarrow}{3} \equiv \tilde{\sigma}_{xy}^{SJ\uparrow} + \tilde{\sigma}_{xy}^{SJ\downarrow}, \quad (48)$$

where δ^s is the transverse displacement (or side jump) given by $\hbar v_F^s/4mc^2 = \lambda^2 k_F^s/4$. The expression of $\tilde{\sigma}_{xy}$ for the side jump is similar to the expression (41) of $\tilde{\sigma}_{xx}$ but instead of the mean-free path l , we have 2δ . In contrast to $\tilde{\sigma}_{xy}^{SS}$, the side-jump contribution to the off-diagonal conductivity is independent of disorder.

In the case of a parabolic band, the Einstein relation (41) reduces to the Drude formula with two spin channels

$$\tilde{\sigma}_{xx} = e^2 \frac{n_\uparrow \tau_F^\uparrow}{m} + e^2 \frac{n_\downarrow \tau_F^\downarrow}{m}, \quad (49)$$

where $n_s = m \mathcal{N}_s (v_F^s)^2/3$ is the electron density for spin s . The skew-scattering (46) and side-jump (48) contributions yield

$$\tilde{\sigma}_{xy}^{SS} = -\frac{e^2 \lambda^2}{2\hbar} \frac{\pi \Omega_0 \langle V^3 \rangle_c}{\hbar \langle V^2 \rangle_c} (n_\uparrow^2 \tau_F^\uparrow - n_\downarrow^2 \tau_F^\downarrow) \quad (50)$$

and

$$\tilde{\sigma}_{xy}^{SJ} = -\frac{e^2 \lambda^2}{2\hbar} (n_\uparrow - n_\downarrow). \quad (51)$$

B. Pauli approach

In the Pauli approach, the Hamiltonian given by Eq. (3) is the sum of a non-perturbed part and a perturbation W given by Eq. (4) which contains the potential and the spin-orbit coupling. The velocity associated with this Hamiltonian consists of a normal part and an anomalous part due to the spin-orbit coupling

$$\mathbf{v} = \frac{\mathbf{p}}{m} + \frac{\hbar}{4m^2 c^2} (\boldsymbol{\sigma} \times \nabla V). \quad (52)$$

The spin-orbit coupling contribution to the life-time is not relevant, then the average Green's function is $\langle k, s | \underline{G}^\pm | k, s \rangle = (\varepsilon_F - \varepsilon_k^s \pm i\hbar/2\tau_k^s)^{-1}$ where τ_k^s is given by Eq. (36). As a consequence, the derivation of the diagonal conductivity $\tilde{\sigma}_{xx}$ is similar to the one done in the Dirac approach and we obtain the expression (41).

The off-diagonal elements of the conductivity are obtained from the vertex corrections. For the skew scattering, the diagrams which contribute are exactly the same than in the Dirac approach (see Fig. 5) because the only matrix elements of the potential (44) which contribute in the Dirac approach correspond precisely to the matrix elements of the potential in the Pauli approach [see Eq. (5)]. The other terms in Eq. (44) are Darwin-like terms and do not contribute to the off-diagonal conductivity. Then, in the Pauli approach,

the skew-scattering mechanism corresponds to the same Feynman diagrams and gives the same final expression (46) as the weak-relativistic limit of the Dirac approach.

Concerning the side jump, the correspondence between the two approaches is not so simple. In the Dirac approach, we have seen that a virtual transition occurs from the upper band to the lower band. In the Pauli approach, no such a transition can take place because there is only one band. However, we have a supplementary part in the velocity, the anomalous velocity which is of order $1/c^2$ and leads to the side-jump mechanism. The corresponding diagrams are depicted on the right column of Fig. 6. For each diagram in the left column (i.e., in the Dirac approach), we have an equivalent diagram in the right column (i.e., in the Pauli approach). The change between the left and right column corresponds to a vertex renormalization because the matrix elements of the product $\mathbf{v} G V$ in the Dirac approach are equal to the matrix elements of \mathbf{v} in the Pauli approach

$$\begin{aligned} \langle k, s | \mathbf{v} | k', s' \rangle &= \frac{\hbar \mathbf{k}}{m} \delta_{kk'} \delta_{ss'} \\ &+ \tilde{V}(\mathbf{k}' - \mathbf{k}) \frac{i\hbar}{4m^2 c^2} \boldsymbol{\sigma}_{ss'} \times (\mathbf{k} - \mathbf{k}'). \end{aligned} \quad (53)$$

Thus, when we calculate, for example, Fig. 6(a')

$$\begin{aligned} \tilde{\sigma}_{xy}^{6(a')} &= \frac{e^2 \hbar}{2\pi \Omega} \sum_{kk's} \langle \langle k, s | v_x | k', s \rangle \rangle^{(2)} \langle k', s | \underline{G}^+ | k', s \rangle^{(0)} \\ &\times \langle k', s | v_y | k', s \rangle^{(0)} \langle k', s | \underline{G}^- | k', s \rangle^{(0)} \\ &\times \langle k', s | V | k, s \rangle^{(0)} \langle k, s | \underline{G}^- | k, s \rangle^{(0)} \rangle_c, \end{aligned} \quad (54)$$

we obtain the same contribution than from the expression (47) of Fig. 6(a). The final result, after summation over Figs. 6(a') to 6(d'), is then identical to Eq. (48).

V. DISCUSSION

We now briefly discuss the influence of impurity scattering and phonon scattering on the resistivity and on the anomalous Hall resistivity, which are, in the limit $\tilde{\sigma}_{xy} \ll \tilde{\sigma}_{xx}$ simply given by $\tilde{\rho}_{xx} \approx 1/\tilde{\sigma}_{xx}$ and $\tilde{\rho}_H = -\tilde{\rho}_{xy} \approx \tilde{\sigma}_{xy}/\tilde{\sigma}_{xx}^2$. The only terms which depend on the scattering in the expressions of $\tilde{\sigma}_{xy}$ given by Eqs. (46) and (48) and of $\tilde{\sigma}_{xx}$ given by (41), are the moments $\langle V^2 \rangle_c$ and $\langle V^3 \rangle_c$. Indeed, we have

$$\left\{ \begin{array}{l} \tilde{\sigma}_{xx} \propto \frac{1}{\langle V^2 \rangle_c}, \\ \tilde{\sigma}_{xy}^{SS} \propto \frac{\langle V^3 \rangle_c}{\langle V^2 \rangle_c^2}, \\ \tilde{\sigma}_{xy}^{SJ} \text{ independent of } \langle V^n \rangle_c. \end{array} \right. \quad (55)$$

Then, the variations with the moments $\langle V^2 \rangle_c$ and $\langle V^3 \rangle_c$ of the resistivity and the anomalous Hall resistivity are similar to $\tilde{\rho}_{xx} \propto \langle V^2 \rangle_c$, $\tilde{\rho}_{xy}^{SS} \propto \langle V^3 \rangle_c$, and $\tilde{\rho}_{xy}^{SJ} \propto \langle V^2 \rangle_c^2$.

To illustrate the dependence with disorder in the case of impurity scattering, we consider a binary alloy $A_x B_{1-x}$ for which

$$\langle V^2 \rangle_c = x(1-x)(\varepsilon_A - \varepsilon_B)^2 \quad (56)$$

and

$$\langle V^3 \rangle_c = x(1-x)(1-2x)(\varepsilon_A - \varepsilon_B)^3, \quad (57)$$

where $\varepsilon_{A(B)}$ is the value of the potential V on site $A(B)$ and x is the concentration of sites A . Keeping the lowest orders in x (weak-disorder limit), we get

$$\begin{cases} \tilde{\rho}_{xx} \propto x, \\ \tilde{\rho}_{xy}^{SS} \propto (x - 3x^2), \\ \tilde{\rho}_{xy}^{SJ} \propto x^2, \end{cases} \quad (58)$$

which is in agreement with the simple relation given by Eq. (2) but in contradiction with the common belief that the quadratic term would arise only from the side-jump mechanism. In fact, the skew-scattering mechanism, which is responsible for the linear term, gives also an important contribution to the quadratic term, a result that Kondorskii *et al.*²³ have already obtained. In addition, our calculations specify all the approximations which founded the relation (2) and show that it should not be valid in the general case, in particular for high-disordered system, high-relativistic limit, complex band structure or in the case of heterogeneous systems, such as thin films or multilayers.

Something may also be said about phonon scattering. Due to the fluctuating sign of the potential generated by phonons, the third moment $\langle V \rangle_c^3$ can be expected to be very small and accordingly, the skew-scattering contribution (46) to the conductivity is negligible.²² We then have

$$\begin{cases} \tilde{\rho}_{xx} \propto \langle V^2 \rangle_c, \\ \tilde{\rho}_{xy}^{SS} \approx 0, \\ \tilde{\rho}_{xy}^{SJ} \propto \langle V^2 \rangle_c^2 \end{cases} \quad (59)$$

which yields the simple relation $\tilde{\rho}_{xy} \propto \tilde{\rho}_{xx}^2$, in agreement with experimental results.³⁰

The Hall angle, which corresponds to the angle between the electric field and the charge current, is an important quantity. For an applied electric field in the x direction and an effective magnetic field in the z direction, we have $\text{tg}(\theta_H) \equiv j_y/j_x = \tilde{\sigma}_{yx}/\tilde{\sigma}_{xx}$. The conductivity elements $\tilde{\sigma}_{xx}$ and $\tilde{\sigma}_{yx}$ are in a first approximation the sums of contributions due to spins up and down. We can thus define a spin-dependent Hall angle

$$\text{tg}(\theta_H^{\uparrow(\downarrow)}) \equiv \frac{j_y^{\uparrow(\downarrow)}}{j_x^{\uparrow(\downarrow)}} = \frac{\tilde{\sigma}_{yx}^{\uparrow(\downarrow)}}{\tilde{\sigma}_{xx}^{\uparrow(\downarrow)}}. \quad (60)$$

We insert expressions (46) and (48) of the skew-scattering and side-jump off-diagonal conductivities as well as expression (41) of the diagonal conductivity and obtain for spin s

$$\theta_H^s \approx s \left(\frac{2\delta^s}{l^s} + \frac{\pi m^2 \lambda^2}{6\hbar^2} \frac{\langle V^3 \rangle_c}{\langle V^2 \rangle_c} \mathcal{N}_s \Omega_0 (v_F^s)^2 \right). \quad (61)$$

θ_H^{\uparrow} and θ_H^{\downarrow} are not only opposite in sign, they take distinct absolute values due to spin polarization. As a consequence, the spin current ($\mathbf{j}^{\uparrow} - \mathbf{j}^{\downarrow}$) has a longitudinal (i.e., along the x axis) and a transverse (i.e., along the y axis) component and the charge current ($\mathbf{j}^{\uparrow} + \mathbf{j}^{\downarrow}$) acquires a transverse component which corresponds to the anomalous Hall effect. In a paramagnetic material, Eq. (61) yields $\theta_H^{\uparrow} = -\theta_H^{\downarrow}$ and both the transverse component of the charge current and the longitudinal component of the spin current vanish. However, the transverse component of the spin current remains. It corresponds precisely to the ‘‘spin Hall effect’’ recently proposed.¹²

In the case of impurity scattering and in the weak-disorder limit, the magnitude of the Hall angle is determined mostly by the skew-scattering contribution. Indeed, in this limit we have $\theta_H^{SJ} \approx 2\delta/l \approx 10^{-3}$ rad whereas $\theta_H^{SS} \approx \pi(1-2x)(\varepsilon_A - \varepsilon_B)\varepsilon_F/3mc^2W \approx 5 \times 10^{-2}$ rad where we have taken $l \approx 200$ Å, $x \approx 0.2$, $\varepsilon_A - \varepsilon_B \approx 2$ eV, $\varepsilon_F \approx 10$ eV, the band width $W \approx 5$ eV, $mc^2 \approx 500$ keV and a band factor $\alpha \approx 10^4$. For simplicity, we have dropped the spin index. This order of magnitude is consistent with experimental results.²² When the disorder increases, the mean-free-path l decreases significantly which means, since the quantity δ is disorder independent, an increase in the side-jump contribution to the Hall angle. However, the skew-scattering contribution to the Hall angle increases in the same way. It is thus not possible to predict in this first approach which contribution is dominant in the high-disorder regime. In the case of phonon scattering, the Hall angle contains mostly the side-jump contribution $\theta_H = \theta_H^{SJ} \approx 2\delta/l$ which is of order $\approx 10^{-2}$ rad where we have used $\delta \approx 10^{-11}$ m and $l = \tau v_F$ with a relaxation time $\tau \approx 10^{-15}$ s and $v_F \approx 10^6$ m s⁻¹.

To summarize, we have, in this article, proposed a model based on the Dirac equation and on the Kubo formalism which allows one to calculate on the same footing the anomalous Hall conductivity due to both skew-scattering and side-jump mechanisms. The consistency of this approach with the one based on the Pauli equation has been studied in detail in the weak-relativistic limit. In particular, we have shown that in order to calculate the anomalous Hall conductivity one has to consider in the Dirac approach the total conductivity $\tilde{\sigma}_{ij}^I + \tilde{\sigma}_{ij}^{II}$, otherwise unphysical results are obtained. Next, we applied our model to treat a disordered ferromagnetic bulk compound submitted to a potential in the free electron approximation, weak-scattering and weak-relativistic limits. By these means, we have obtained explicit expressions for the anomalous Hall conductivity for both skew-scattering and side-jump mechanisms [given by Eqs. (46) and (48)]. In addition, we have highlighted the difference concerning the Feynman diagrams describing the side-

jump mechanism in the Dirac and Pauli approaches and have shown that it corresponds to different vertex renormalizations.

APPENDIX A: FROM THE KUBO FORMULA TO THE STREDA FORMULA

In the linear response approximation, Kubo has shown that the conductivity tensor is related to a two currents correlation function³⁵

$$\tilde{\sigma}_{ij}(\omega) = \Omega \lim_{s \rightarrow 0^+} \int_0^\beta d\lambda \int_0^{+\infty} dt e^{(it/\hbar)(-\hbar\omega + is)} \times \text{Tr} \langle \rho_0 J_j(0) J_i(t + i\hbar\lambda) \rangle_c, \quad (\text{A1})$$

where it is assumed that the applied field leads to a time-dependent perturbation of the form $H'(t) = H'_0 \exp[it/\hbar(-\hbar\omega + is)]$. Ω is the volume of the sample, $\beta \equiv 1/k_B T$, ρ_0 is the density matrix in equilibrium in absence of perturbation, J_i is the i component of the current density operator in the Heisenberg representation, and $\langle \dots \rangle_c$ denotes the configurational average. Following Luttinger,³⁶ we obtain in the independent electrons approximation

$$\langle n | J_i(t + i\hbar\lambda) | m \rangle = e^{(i/\hbar)(t + i\hbar\lambda)(\varepsilon_n - \varepsilon_m)} \langle n | \tilde{J}_i | m \rangle, \quad (\text{A2})$$

where we have used $H = \sum_n \varepsilon_n a_n^\dagger a_n$ and defined \tilde{J} as the current density operator in the Schrödinger representation. Using the relation $\text{Tr}[\rho_0 a_m^\dagger a_n a_p^\dagger a_q] = \delta_{mq} \delta_{np} f(\varepsilon_m) [1 - f(\varepsilon_n)]$ where $f(\varepsilon)$ is the Fermi-Dirac distribution function, we get

$$\begin{aligned} \tilde{\sigma}_{ij}(\omega) &= \Omega \lim_{s \rightarrow 0^+} \int_0^\beta d\lambda e^{-\lambda(\varepsilon_n - \varepsilon_m)} \\ &\times \int_0^{+\infty} dt \sum_{nm} \langle f(\varepsilon_m) (1 - f(\varepsilon_n)) \rangle \\ &\times e^{(it/\hbar)(-\hbar\omega + is + \varepsilon_n - \varepsilon_m)} \langle m | \tilde{J}_j | n \rangle \langle n | \tilde{J}_i | m \rangle \rangle_c. \end{aligned} \quad (\text{A3})$$

The integration over λ leads to a factor $(1 - e^{-\beta(\varepsilon_n - \varepsilon_m)})/(\varepsilon_n - \varepsilon_m)$ which can be simplified with $f(\varepsilon_m) [1 - f(\varepsilon_n)]$ as

$$\frac{1 - e^{-\beta(\varepsilon_n - \varepsilon_m)}}{\varepsilon_n - \varepsilon_m} f(\varepsilon_m) [1 - f(\varepsilon_n)] = \frac{f(\varepsilon_m) - f(\varepsilon_n)}{\varepsilon_n - \varepsilon_m}. \quad (\text{A4})$$

Inserting this in Eq. (A3) and performing the integration over t , we obtain

$$\begin{aligned} \tilde{\sigma}_{ij}(\omega) &= i\hbar\Omega \lim_{s \rightarrow 0^+} \sum_{nm} \left\langle \frac{f(\varepsilon_m) - f(\varepsilon_n)}{(\varepsilon_n - \varepsilon_m)(\varepsilon_n - \varepsilon_m - \hbar\omega + is)} \right. \\ &\left. \times \langle m | \tilde{J}_j | n \rangle \langle n | \tilde{J}_i | m \rangle \right\rangle_c. \end{aligned} \quad (\text{A5})$$

We shall now make some transformations of this expression in order to get the Bastin formula.

We restrict our derivation to zero frequency (from now, we drop the ω variable). After inserting the identity $\int_{-\infty}^{+\infty} d\varepsilon \delta(\varepsilon - H) = 1$ in Eq. (A5), we obtain

$$\begin{aligned} \tilde{\sigma}_{ij} &= i\hbar\Omega \lim_{s \rightarrow 0^+} \int_{-\infty}^{+\infty} d\varepsilon \sum_{nm} \left\langle \left(\frac{f(\varepsilon) \delta(\varepsilon - \varepsilon_m)}{(\varepsilon_n - \varepsilon)(\varepsilon_n - \varepsilon + is)} \right. \right. \\ &\left. \left. - \frac{f(\varepsilon) \delta(\varepsilon - \varepsilon_n)}{(\varepsilon - \varepsilon_m)(\varepsilon - \varepsilon_m + is)} \right) \langle m | \tilde{J}_j | n \rangle \langle n | \tilde{J}_i | m \rangle \right\rangle_c. \end{aligned} \quad (\text{A6})$$

We remark that

$$\lim_{s \rightarrow 0^+} \frac{1}{(\varepsilon_n - \varepsilon)(\varepsilon_n - \varepsilon + is)} = \lim_{s \rightarrow 0^+} \frac{d}{d\varepsilon} \left(\frac{1}{\varepsilon_n - \varepsilon + is} \right); \quad (\text{A7})$$

then we have

$$\begin{aligned} \tilde{\sigma}_{ij} &= -i\hbar\Omega \lim_{s \rightarrow 0^+} \int_{-\infty}^{+\infty} d\varepsilon f(\varepsilon) \\ &\times \sum_{nm} \left\langle \langle m | \tilde{J}_j | n \rangle \frac{d}{d\varepsilon} \left(\frac{1}{\varepsilon - \varepsilon_n - is} \right) \langle n | \tilde{J}_i | m \rangle \delta(\varepsilon - \varepsilon_m) \right. \\ &\left. - \langle m | \tilde{J}_j | n \rangle \delta(\varepsilon - \varepsilon_n) \langle n | \tilde{J}_i | m \rangle \frac{d}{d\varepsilon} \left(\frac{1}{\varepsilon - \varepsilon_m + is} \right) \right\rangle_c, \end{aligned} \quad (\text{A8})$$

which can be expressed as

$$\begin{aligned} \tilde{\sigma}_{ij} &= \frac{ie^2\hbar}{\Omega} \int_{-\infty}^{+\infty} d\varepsilon f(\varepsilon) \\ &\times \text{Tr} \left\langle v_i \frac{dG^+(\varepsilon)}{d\varepsilon} v_j \delta(\varepsilon - H) - v_i \delta(\varepsilon - H) v_j \frac{dG^-(\varepsilon)}{d\varepsilon} \right\rangle_c, \end{aligned} \quad (\text{A9})$$

where we have introduced the Green's function $G^\pm(\varepsilon) = \lim_{s \rightarrow 0^+} (\varepsilon - H \pm is)^{-1}$ and the velocity through the relation $\tilde{\mathbf{J}} = -e\mathbf{v}/\Omega$. This expression for the conductivity was first obtained by Bastin *et al.*³⁷ but in the particular case of a

Schrödinger Hamiltonian and made explicit use of the form taken by the velocity operator in the Schrödinger case. The present derivation is more general in the sense that it is independent of the explicit form of the velocity operator and is therefore valid both for the Schrödinger, Pauli, and Dirac cases. The only restriction is the independent electrons approximation. This formula, called Bastin formula, is interesting because it expresses the conductivity as a product of velocities and Green's functions. However, it is still difficult to calculate because of the integration over the energy ε . By making an integration by parts, a factor $df(\varepsilon)/d\varepsilon$ appears instead of the factor $f(\varepsilon)$ and the integration interval will be thus reduced.

In Eq. (A9), we express the delta function in terms of Green's functions using $\delta(\varepsilon - H) = -(G^+(\varepsilon) - G^-(\varepsilon))/2i\pi$. We keep one half of this expression and make an integration by parts on the second half, then we get

$$\begin{aligned} \tilde{\sigma}_{ij} = & -\frac{e^2\hbar}{4\pi\Omega} \int_{-\infty}^{+\infty} d\varepsilon \frac{df(\varepsilon)}{d\varepsilon} \text{Tr} \langle v_i (G^+(\varepsilon) \\ & - G^-(\varepsilon)) v_j G^-(\varepsilon) - v_i G^+(\varepsilon) v_j (G^+(\varepsilon) - G^-(\varepsilon)) \rangle_c \\ & + \frac{e^2\hbar}{4\pi\Omega} \int_{-\infty}^{+\infty} d\varepsilon f(\varepsilon) \text{Tr} \left\langle v_i \frac{dG^-(\varepsilon)}{d\varepsilon} v_j G^-(\varepsilon) \right. \\ & - v_i G^-(\varepsilon) v_j \frac{dG^-(\varepsilon)}{d\varepsilon} + v_i G^+(\varepsilon) v_j \frac{dG^+(\varepsilon)}{d\varepsilon} \\ & \left. - v_i \frac{dG^+(\varepsilon)}{d\varepsilon} v_j G^+(\varepsilon) \right\rangle_c. \end{aligned} \quad (\text{A10})$$

The second term in this expression can be simplified by using the relations $dG^\pm(\varepsilon)/d\varepsilon = -[G^\pm(\varepsilon)]^2$ and $i\hbar v_i = [r_i, H] = -[r_i, G^{-1}]$ and by performing once more an integration by parts. Finally, the conductivity can be written as a sum of two terms $\tilde{\sigma}_{ij} = \tilde{\sigma}_{ij}^I + \tilde{\sigma}_{ij}^{II}$ where

$$\begin{aligned} \tilde{\sigma}_{ij}^I = & -\frac{e^2\hbar}{4\pi\Omega} \int_{-\infty}^{+\infty} d\varepsilon \frac{df(\varepsilon)}{d\varepsilon} \text{Tr} \langle v_i (G^+(\varepsilon) \\ & - G^-(\varepsilon)) v_j G^-(\varepsilon) - v_i G^+(\varepsilon) v_j (G^+(\varepsilon) - G^-(\varepsilon)) \rangle_c \end{aligned} \quad (\text{A11})$$

and

$$\begin{aligned} \tilde{\sigma}_{ij}^{II} = & \frac{e^2}{4i\pi\Omega} \int_{-\infty}^{+\infty} d\varepsilon \frac{df(\varepsilon)}{d\varepsilon} \\ & \times \text{Tr} \langle (G^+(\varepsilon) - G^-(\varepsilon)) (r_i v_j - r_j v_i) \rangle_c. \end{aligned} \quad (\text{A12})$$

Equations (A11) and (A12) correspond to the formula obtained by Streda³⁸ in the Schrödinger case. The present derivation shows that it holds also in the Pauli and Dirac cases.

For the diagonal components of the conductivity tensor, $\tilde{\sigma}_{ij}^{II}$ is equal to zero and we obtain the Kubo-Greenwood formula²⁹

$$\begin{aligned} \tilde{\sigma}_{ii} = & \frac{e^2\hbar}{4\pi\Omega} \int_{-\infty}^{+\infty} d\varepsilon \frac{df(\varepsilon)}{d\varepsilon} \text{Tr} \langle v_i (G^+(\varepsilon) - G^-(\varepsilon)) \\ & \times v_i (G^+(\varepsilon) - G^-(\varepsilon)) \rangle_c. \end{aligned} \quad (\text{A13})$$

At zero temperature, the factor $df(\varepsilon)/d\varepsilon$ is equal to $-\delta(\varepsilon - \varepsilon_F)$, only electrons at the Fermi level contribute to the conductivity (for both diagonal and off-diagonal components). In conclusion, at $\omega=0$ and $T=0$, the conductivity tensor can be expressed as a sum of two terms $\tilde{\sigma}_{ij} = \tilde{\sigma}_{ij}^I + \tilde{\sigma}_{ij}^{II}$ with

$$\tilde{\sigma}_{ij}^I = \frac{e^2\hbar}{4\pi\Omega} \text{Tr} \langle v_i (G^+ - G^-) v_j G^- - v_i G^+ v_j (G^+ - G^-) \rangle_c \quad (\text{A14})$$

and

$$\tilde{\sigma}_{ij}^{II} = -\frac{e^2}{4i\pi\Omega} \text{Tr} \langle (G^+ - G^-) (r_i v_j - r_j v_i) \rangle_c, \quad (\text{A15})$$

where we have dropped the energy reference ε_F by introducing the Green's functions at the Fermi level $G^\pm = G(\varepsilon_F \pm i0) = (\varepsilon_F \pm i0 - H)^{-1}$.

APPENDIX B: STREDA FORMULA IN THE WEAK-RELATIVISTIC LIMIT

In this appendix, we give the detail of the calculation concerning the weak-relativistic expansion of the Streda conductivity starting from the Dirac equation. From Eq. (A14), we see that $\tilde{\sigma}_{ij}^I$ is a combination of terms such as

$$\Lambda_{ij}(z_1, z_2) = \frac{e^2\hbar}{4\pi\Omega} \text{Tr} \langle v_i G(z_1) v_j G(z_2) \rangle_c, \quad (\text{B1})$$

where z_1 and z_2 are equals to $\varepsilon_F \pm i0$. When we insert the Dirac velocity (17) and the Dirac Green's function (19) in Eq. (B1), make the explicit product of the four operators and take the trace over the lower and upper components of the wave function, we obtain the general form

$$\begin{aligned}
\Lambda_{ij}(z_1, z_2) = & \frac{e^2 \hbar}{4\pi\Omega} \text{Tr} \left\langle \sigma_i D(z_1) \frac{\boldsymbol{\sigma} \cdot \mathbf{p}}{2m} \tilde{G}(z_1) \sigma_j D(z_2) \frac{\boldsymbol{\sigma} \cdot \mathbf{p}}{2m} \tilde{G}(z_2) \right. \\
& + \sigma_i \tilde{G}(z_1) \frac{\boldsymbol{\sigma} \cdot \mathbf{p}}{2m} Q^{-1}(z_1) D(z_1) Q(z_1) \sigma_j \tilde{G}(z_2) \frac{\boldsymbol{\sigma} \cdot \mathbf{p}}{2m} Q^{-1}(z_2) D(z_2) Q(z_2) \\
& + \sigma_i D(z_1) \left(\frac{1}{2m} + \frac{\boldsymbol{\sigma} \cdot \mathbf{p}}{2m} \tilde{G}(z_1) \frac{\boldsymbol{\sigma} \cdot \mathbf{p}}{2m} \right) \sigma_j \left(\tilde{G}(z_2) - \tilde{G}(z_2) \frac{\boldsymbol{\sigma} \cdot \mathbf{p}}{2mc} [z_2 - V - \mu_B (\boldsymbol{\sigma} \cdot \mathbf{B}_{\text{eff}})] D(z_2) \frac{\boldsymbol{\sigma} \cdot \mathbf{p}}{2mc} \tilde{G}(z_2) \right) \\
& \left. + \sigma_i \left(\tilde{G}(z_1) - \tilde{G}(z_1) \frac{\boldsymbol{\sigma} \cdot \mathbf{p}}{2mc} [z_1 - V - \mu_B (\boldsymbol{\sigma} \cdot \mathbf{B}_{\text{eff}})] D(z_1) \frac{\boldsymbol{\sigma} \cdot \mathbf{p}}{2mc} \tilde{G}(z_1) \right) \sigma_j D(z_2) \left(\frac{1}{2m} + \frac{\boldsymbol{\sigma} \cdot \mathbf{p}}{2m} \tilde{G}(z_2) \frac{\boldsymbol{\sigma} \cdot \mathbf{p}}{2m} \right) \right\rangle_c.
\end{aligned} \tag{B2}$$

Similarly, when we insert Eqs. (17) and (19) in Eq. (A15), we get

$$\begin{aligned}
\tilde{\sigma}_{ij}^H = & -\frac{e^2}{4i\pi\Omega} \text{Tr} \left\langle \left(\tilde{G}^+ \frac{\boldsymbol{\sigma} \cdot \mathbf{p}}{2m} (Q^+)^{-1} D^+ Q^+ + D^+ \frac{\boldsymbol{\sigma} \cdot \mathbf{p}}{2m} \tilde{G}^+ \right. \right. \\
& \left. \left. - \tilde{G}^- \frac{\boldsymbol{\sigma} \cdot \mathbf{p}}{2m} (Q^-)^{-1} D^- Q^- - D^- \frac{\boldsymbol{\sigma} \cdot \mathbf{p}}{2m} \tilde{G}^- \right) (r_i \sigma_j - r_j \sigma_i) \right\rangle_c.
\end{aligned} \tag{B3}$$

Expressions (B2) and (B3) are exact expressions without any assumption on the value of c . We will now calculate the weak-relativistic expansion of these expressions at orders $1/c^0$ and $1/c^2$ in order to compare them with the expression obtained from the Pauli approach.

1. Dirac conductivity at order $1/c^0$

In the nonrelativistic limit, D is simply equal to the unit matrix [see Eq. (20)], thus Eq. (B2) can be rewritten as

$$\begin{aligned}
\Lambda_{ij}^{(0)}(z_1, z_2) = & \frac{e^2 \hbar}{4\pi\Omega} \text{Tr} \left\langle \frac{p_i}{m} \tilde{G}(z_1) \frac{p_j}{m} \tilde{G}(z_2) \right. \\
& \left. + \frac{1}{2m} (\sigma_i \sigma_j \tilde{G}(z_2) + \sigma_j \sigma_i \tilde{G}(z_1)) \right\rangle_c,
\end{aligned} \tag{B4}$$

where we have used the fact that $\sigma_i (\boldsymbol{\sigma} \cdot \mathbf{p}) + (\boldsymbol{\sigma} \cdot \mathbf{p}) \sigma_i = 2p_i$. When we insert this expression in Eq. (A14), the conductivity $\tilde{\sigma}_{ij}^I$ at order $1/c^0$ is

$$\begin{aligned}
\tilde{\sigma}_{ij}^{I(0)} = & \frac{e^2 \hbar}{4\pi\Omega} \text{Tr} \left\langle \frac{p_i}{m} (\tilde{G}^+ - \tilde{G}^-) \frac{p_j}{m} \tilde{G}^- - \frac{p_i}{m} \tilde{G}^+ + \frac{p_j}{m} (\tilde{G}^+ \right. \\
& \left. - \tilde{G}^-) \right\rangle_c + \varepsilon_{ijk} \frac{e^2 \hbar}{4i\pi m \Omega} \text{Tr} \langle \sigma_k (\tilde{G}^+ - \tilde{G}^-) \rangle_c,
\end{aligned} \tag{B5}$$

where $\varepsilon_{ijk} = 1$ if $\{i, j, k\} = \{x, y, z\}$ or cyclic permutations and $\varepsilon_{ijk} = 0$ otherwise. This factor is introduced through the term

$(\sigma_i \sigma_j - \sigma_j \sigma_i) = 2i\varepsilon_{ijk} \sigma_k$. The first term on the right hand side corresponds exactly to the contribution that we get in a nonrelativistic description because in this case the velocity is $\tilde{\mathbf{v}} = \mathbf{p}/m$ and the Green's function is simply the nonrelativistic Green's function \tilde{G} . In contrast, the second term is not present in the Pauli approach and should not appear when we take the non-relativistic limit in the Dirac approach. In fact, we show below that this term is exactly cancelled by an opposite term in $\tilde{\sigma}_{ij}^{I(0)}$. Replacing D by 1 in Eq. (B3), we get $\tilde{\sigma}_{ij}^H$ at order $1/c^0$

$$\begin{aligned}
\tilde{\sigma}_{ij}^{H(0)} = & -\frac{e^2}{4i\pi\Omega} \text{Tr} \left\langle (\tilde{G}^+ - \tilde{G}^-) \left(r_i \frac{p_j}{m} - r_j \frac{p_i}{m} \right) \right\rangle_c \\
& - \varepsilon_{ijk} \frac{e^2 \hbar}{4i\pi m \Omega} \text{Tr} \langle \sigma_k (\tilde{G}^+ - \tilde{G}^-) \rangle_c,
\end{aligned} \tag{B6}$$

where we have used the relations $(\boldsymbol{\sigma} \cdot \mathbf{A})(\boldsymbol{\sigma} \cdot \mathbf{B}) = (\mathbf{A} \cdot \mathbf{B}) + i\boldsymbol{\sigma}(\mathbf{A} \times \mathbf{B})$ and $[r_i, p_j] = i\hbar \delta_{ij}$. The second term in the right hand side cancels the supplementary term in Eq. (B5) and we obtain finally for the total Dirac conductivity at order $1/c^0$

$$\begin{aligned}
\tilde{\sigma}_{ij}^{(0)} = & \tilde{\sigma}_{ij}^{I(0)} + \tilde{\sigma}_{ij}^{H(0)} \\
= & \frac{e^2 \hbar}{4\pi\Omega} \text{Tr} \left\langle \frac{p_i}{m} (\tilde{G}^+ - \tilde{G}^-) \frac{p_j}{m} \tilde{G}^- \right. \\
& \left. - \frac{p_i}{m} \tilde{G}^+ + \frac{p_j}{m} (\tilde{G}^+ - \tilde{G}^-) \right\rangle_c \\
& - \frac{e^2}{4i\pi\Omega} \text{Tr} \left\langle (\tilde{G}^+ - \tilde{G}^-) \left(r_i \frac{p_j}{m} - r_j \frac{p_i}{m} \right) \right\rangle_c,
\end{aligned} \tag{B7}$$

which corresponds exactly to the total conductivity obtained from Eqs. (A14) and (A15) when we insert the nonrelativistic Pauli velocity $\tilde{\mathbf{v}} = \mathbf{p}/m$ and the nonrelativistic Pauli Green's function \tilde{G} .

2. Dirac conductivity at order $1/c^2$

To get $\tilde{\sigma}_{ij}$ at order $1/c^2$, it is necessary to take into account the next terms in the expansion of D given by Eq. (20): $D(z) \approx 1 - Q(z)[z - V - \mu_B(\boldsymbol{\sigma} \cdot \mathbf{B}_{\text{eff}})]/2mc^2$. Thus, from Eq. (B2), we get

$$\begin{aligned}
\Lambda_{ij}^{(2)}(z_1, z_2) = & \frac{e^2 \hbar}{4\pi\Omega} \text{Tr} \left\langle \frac{p_i}{m} \tilde{G}(z_1) (\mathbf{v}_{rc})_j \tilde{G}(z_2) + (\mathbf{v}_{rc})_i \tilde{G}(z_1) \frac{p_j}{m} \tilde{G}(z_2) + \frac{p_i}{m} \tilde{G}(z_1) \frac{p_j}{m} \tilde{G}(z_2) H_{rc} \tilde{G}(z_2) \right. \\
& + \frac{p_i}{m} \tilde{G}(z_1) H_{rc} \tilde{G}(z_1) \frac{p_j}{m} \tilde{G}(z_2) - \frac{1}{8m^3 c^2} \{ \sigma_i \sigma_j \tilde{G}(z_2) \boldsymbol{\sigma} \cdot \mathbf{p} [z_2 - V - \mu_B(\boldsymbol{\sigma} \cdot \mathbf{B}_{\text{eff}})] \boldsymbol{\sigma} \cdot \mathbf{p} \tilde{G}(z_2) \\
& + \sigma_j \sigma_i \tilde{G}(z_1) \boldsymbol{\sigma} \cdot \mathbf{p} [z_1 - V - \mu_B(\boldsymbol{\sigma} \cdot \mathbf{B}_{\text{eff}})] \boldsymbol{\sigma} \cdot \mathbf{p} \tilde{G}(z_1) \} - \frac{1}{2m^3 c^2} p_i p_j (\tilde{G}(z_1) + \tilde{G}(z_2)) \\
& - \frac{1}{4m^2 c^2} \{ \sigma_i [z_1 - V - \mu_B(\boldsymbol{\sigma} \cdot \mathbf{B}_{\text{eff}})] \sigma_j \tilde{G}(z_2) + \sigma_j [z_2 - V - \mu_B(\boldsymbol{\sigma} \cdot \mathbf{B}_{\text{eff}})] \sigma_i \tilde{G}(z_1) \} \\
& \left. - \frac{i}{4m^3 c^2} (z_1 - z_2) ((\mathbf{p} \times \boldsymbol{\sigma})_i \tilde{G}(z_1) p_j \tilde{G}(z_2) - p_i \tilde{G}(z_1) (\mathbf{p} \times \boldsymbol{\sigma})_j \tilde{G}(z_2)) \right\rangle_c, \tag{B8}
\end{aligned}$$

where H_{rc} and \mathbf{v}_{rc} are the relativistic corrections at order $1/c^2$ to the Hamiltonian and the velocity respectively given by Eqs. (13) and (14). The last term on the right-hand side does not contribute because $(z_1 - z_2) \rightarrow 0$. Inserting the expression (B8) in the conductivity (A14), we get $\tilde{\sigma}_{ij}^I$ at order $1/c^2$

$$\begin{aligned}
\tilde{\sigma}_{ij}^{I(2)} = & \frac{e^2 \hbar}{4\pi\Omega} \text{Tr} \left\langle (\mathbf{v}_{rc})_i (\tilde{G}^+ - \tilde{G}^-) \frac{p_j}{m} \tilde{G}^- - (\mathbf{v}_{rc})_j \tilde{G}^+ \frac{p_i}{m} (\tilde{G}^+ - \tilde{G}^-) + \frac{p_i}{m} (\tilde{G}^+ - \tilde{G}^-) (\mathbf{v}_{rc})_j \tilde{G}^- \right. \\
& - \frac{p_i}{m} \tilde{G}^+ (\mathbf{v}_{rc})_j (\tilde{G}^+ - \tilde{G}^-) + \frac{p_i}{m} (\tilde{G}^+ H_{rc} \tilde{G}^+ - \tilde{G}^- H_{rc} \tilde{G}^-) \frac{p_j}{m} \tilde{G}^- + \frac{p_i}{m} (\tilde{G}^+ - \tilde{G}^-) \frac{p_j}{m} \tilde{G}^- H_{rc} \tilde{G}^- \\
& \left. - \frac{p_i}{m} \tilde{G}^+ H_{rc} \tilde{G}^+ \frac{p_j}{m} (\tilde{G}^+ - \tilde{G}^-) - \frac{p_i}{m} \tilde{G}^- \frac{p_j}{m} (\tilde{G}^+ H_{rc} \tilde{G}^+ - \tilde{G}^- H_{rc} \tilde{G}^-) \right\rangle_c \\
& - \varepsilon_{ijk} \frac{e^2 \hbar}{16i\pi m^3 c^2 \Omega} \text{Tr} \langle \{ \tilde{G}^+ \boldsymbol{\sigma} \cdot \mathbf{p} [\varepsilon_F - V - \mu_B(\boldsymbol{\sigma} \cdot \mathbf{B}_{\text{eff}})] \boldsymbol{\sigma} \cdot \mathbf{p} \tilde{G}^+ - \tilde{G}^- \boldsymbol{\sigma} \cdot \mathbf{p} [\varepsilon_F - V - \mu_B(\boldsymbol{\sigma} \cdot \mathbf{B}_{\text{eff}})] \boldsymbol{\sigma} \cdot \mathbf{p} \tilde{G}^- \} \sigma_k \rangle_c \\
& + \frac{e^2 \hbar}{16\pi m^2 c^2 \Omega} \text{Tr} \langle (\tilde{G}^+ - \tilde{G}^-) \{ \sigma_i [\varepsilon_F - V - \mu_B(\boldsymbol{\sigma} \cdot \mathbf{B}_{\text{eff}})] \sigma_j - \sigma_j [\varepsilon_F - V - \mu_B(\boldsymbol{\sigma} \cdot \mathbf{B}_{\text{eff}})] \sigma_i \} \rangle_c. \tag{B9}
\end{aligned}$$

The first term corresponds exactly to the relativistic corrections that we get at order $1/c^2$ in the Pauli approach. The two last terms are supplementary terms which should not appear. We show that they are cancelled by terms in $\tilde{\sigma}_{ij}^{II(2)}$. Indeed, when we expand D up to the second order in $1/c$ in the expression (B3) of $\tilde{\sigma}_{ij}^{II}$, we obtain

$$\begin{aligned}
\tilde{\sigma}_{ij}^{II(2)} = & - \frac{e^2}{4i\pi\Omega} \text{Tr} \left\langle (\tilde{G}^+ H_{rc} \tilde{G}^+ - \tilde{G}^- H_{rc} \tilde{G}^-) \left(r_i \frac{p_j}{m} - r_j \frac{p_i}{m} \right) + (\tilde{G}^+ - \tilde{G}^-) [r_i (\mathbf{v}_{rc})_j - r_j (\mathbf{v}_{rc})_i] \right\rangle_c \\
& + \varepsilon_{ijk} \frac{e^2 \hbar}{16i\pi m^3 c^2 \Omega} \text{Tr} \langle \{ \tilde{G}^+ \boldsymbol{\sigma} \cdot \mathbf{p} [\varepsilon_F - V - \mu_B(\boldsymbol{\sigma} \cdot \mathbf{B}_{\text{eff}})] \boldsymbol{\sigma} \cdot \mathbf{p} \tilde{G}^+ - \tilde{G}^- \boldsymbol{\sigma} \cdot \mathbf{p} [\varepsilon_F - V - \mu_B(\boldsymbol{\sigma} \cdot \mathbf{B}_{\text{eff}})] \boldsymbol{\sigma} \cdot \mathbf{p} \tilde{G}^- \} \sigma_k \rangle_c \\
& - \frac{e^2 \hbar}{16\pi m^2 c^2 \Omega} \text{Tr} \langle (\tilde{G}^+ - \tilde{G}^-) \{ \sigma_i [\varepsilon_F - V - \mu_B(\boldsymbol{\sigma} \cdot \mathbf{B}_{\text{eff}})] \sigma_j - \sigma_j [\varepsilon_F - V - \mu_B(\boldsymbol{\sigma} \cdot \mathbf{B}_{\text{eff}})] \sigma_i \} \rangle_c. \tag{B10}
\end{aligned}$$

The two last terms on the right-hand side cancel the supplementary terms in Eq. (B9) and we obtain finally for the total conductivity at order $1/c^2$

$$\begin{aligned}
\tilde{\sigma}_{ij}^{(2)} = \tilde{\sigma}_{ij}^{I(2)} + \tilde{\sigma}_{ij}^{II(2)} = \frac{e^2 \hbar}{4\pi\Omega} \text{Tr} & \left((\mathbf{v}_{rc})_i (\tilde{G}^+ - \tilde{G}^-) \frac{P_j}{m} \tilde{G}^- - (\mathbf{v}_{rc})_i \tilde{G}^+ \frac{P_j}{m} (\tilde{G}^+ - \tilde{G}^-) + \frac{P_i}{m} (\tilde{G}^+ - \tilde{G}^-) (\mathbf{v}_{rc})_j \tilde{G}^- \right. \\
& - \frac{P_i}{m} \tilde{G}^+ (\mathbf{v}_{rc})_j (\tilde{G}^+ - \tilde{G}^-) + \frac{P_i}{m} (\tilde{G}^+ H_{rc} \tilde{G}^+ - \tilde{G}^- H_{rc} \tilde{G}^-) \frac{P_j}{m} \tilde{G}^- + \frac{P_i}{m} (\tilde{G}^+ - \tilde{G}^-) \frac{P_j}{m} \tilde{G}^- H_{rc} \tilde{G}^- \\
& \left. - \frac{P_i}{m} \tilde{G}^+ H_{rc} \tilde{G}^+ \frac{P_j}{m} (\tilde{G}^+ - \tilde{G}^-) - \frac{P_i}{m} \tilde{G}^+ \frac{P_j}{m} (\tilde{G}^+ H_{rc} \tilde{G}^+ - \tilde{G}^- H_{rc} \tilde{G}^-) \right) \\
& - \frac{e^2}{4i\pi\Omega} \text{Tr} \left((\tilde{G}^+ H_{rc} \tilde{G}^+ - \tilde{G}^- H_{rc} \tilde{G}^-) \left(r_i \frac{P_j}{m} - r_j \frac{P_i}{m} \right) + (\tilde{G}^+ - \tilde{G}^-) [r_i (\mathbf{v}_{rc})_j - r_j (\mathbf{v}_{rc})_i] \right) . \quad (\text{B11})
\end{aligned}$$

This expression corresponds exactly to the one that we get from the Pauli approach when we report the Pauli velocity at order $1/c^2$, \mathbf{v}_{rc} , and the Pauli Hamiltonian at order $1/c^2$, H_{rc} , in Eqs. (A14) and (A15). For higher order terms (say of order $1/c^{2n}$ with $n > 1$), we can predict that similar cancellations occur when we consider the total conductivity $\tilde{\sigma}_{ij}^{I(2n)} + \tilde{\sigma}_{ij}^{II(2n)}$. We have thus proved in this appendix the consistency between the Pauli conductivity and the weak-relativistic limit of the Dirac conductivity.

*Electronic address: crepieux@mpi-halle.mpg.de

¹F. P. Beitel and E. M. Pugh, Phys. Rev. **112**, 1516 (1958).

²H. Ashworth, D. Sengupta, G. Schnakenberg, L. Shapiro, and L. Berger, Phys. Rev. **185**, 792 (1969).

³A. K. Majumdar and L. Berger, Phys. Rev. B **7**, 4203 (1973).

⁴R. C. O'Handley, Phys. Rev. B **18**, 2577 (1978).

⁵A. Sinha and A. K. Majumdar, J. Appl. Phys. **50**, 7533 (1979).

⁶A. B. Pakhomov, X. Yan, N. Wang, X. N. Jing, B. Zhao, K. K. Fng, J. Xhie, T. F. Hng, and S. K. Wong, Physica A **241**, 344 (1997); J. C. Denardin, A. B. Pakhomov, M. Knobel, H. Liu, and X. X. Zhang, J. Phys.: Condens. Matter **12**, 3397 (2000).

⁷J. Caulet, C. Train, V. Mathet, R. Laval, B. Bartenlian, P. Veillet, K. Le Dang, and C. Chappert, J. Magn. Magn. Mater. **198**, 318 (1999).

⁸H. Sato, T. Kumano, Y. Aoki, T. Kaneko, and R. Yamamoto, J. Phys. Soc. Jpn. **62**, 416 (1993); C. L. Canedy, X. W. Li, and G. Xiao, J. Appl. Phys. **81**, 5367 (1997); C. L. Canedy, X. W. Li, and G. Xiao, Phys. Rev. B **62**, 508 (2000).

⁹H. Ohno, D. Chiba, F. Matsukura, T. Omiya, E. Abe, T. Dietl, Y. Ohno, and K. Ohtani, Nature (London) **408**, 944 (2000).

¹⁰J. Wunderlich, D. Ravelosona, C. Chappert, F. Cayssol, V. Mathet, J. Ferre, J.-P. Jamet, and A. Thiaville (private communication).

¹¹S. de Haan and J. C. Lodder, J. Magn. Magn. Mater. **168**, 321 (1997); S. Nagagawa, K. Takayama, A. Sato, and M. Naoe, J. Appl. Phys. **85**, 4592 (1999); S. Nagagawa, A. Sato, I. Sasaki, and M. Naoe, *ibid.* **87**, 5705 (2000).

¹²J. E. Hirsch, Phys. Rev. Lett. **83**, 1834 (1999); S. Zhang, *ibid.* **85**, 393 (2000).

¹³R. Karplus and J. M. Luttinger, Phys. Rev. **95**, 1154 (1954).

¹⁴J. Smit, Physica (Amsterdam) **21**, 877 (1955); **24**, 39 (1958).

¹⁵J. M. Luttinger, Phys. Rev. **112**, 739 (1958).

¹⁶L. Berger, Phys. Rev. B **2**, 4559 (1970); **5**, 1862 (1972).

¹⁷J. Smit, Phys. Rev. B **8**, 2349 (1973); L. Berger, *ibid.* **8**, 2351 (1973).

¹⁸S. K. Lyo and T. Holstein, Phys. Rev. B **9**, 2412 (1974).

¹⁹J. Smit, Phys. Rev. B **17**, 1450 (1978); L. Berger, *ibid.* **17**, 1453 (1978).

²⁰P. Nozières and C. Lewiner, J. Phys. (France) **34**, 901 (1973); C.

Lewiner, O. Betbeder-Matibet, and P. Nozières, J. Phys. Chem. Solids **34**, 765 (1973).

²¹S. K. Lyo and T. Holstein, Phys. Rev. Lett. **29**, 423 (1972).

²²L. Berger and G. Bergamann, *The Hall Effect and its Applications*, edited by C. L. Chien and C. R. Westgate (Plenum, New York, 1980), p. 55.

²³YE. I. Kondorskii, A. V. Vedyayev, and A. B. Granovskii, Fiz. Met. Metalloved. **40**, 455 (1975); **40**, 903 (1975); A. N. Voloshinskiy and N. V. Ryzhanova, *ibid.* **34**, 15 (1972).

²⁴A. H. MacDonald and S. H. Vosko, J. Phys. C **12**, 2977 (1979).

²⁵Equation (16) is actually an approximate form of the Kohn-Sham-Dirac equation $H = c \boldsymbol{\alpha} \cdot (\mathbf{p} - e\mathbf{A}) + \beta mc^2 + V$; an approximation generally used to treat relativistic effects in magnetic materials. The calculations presented in Sec. III and Appendix B have also been performed starting from the Kohn-Sham-Dirac equation, in particular the check of the Dirac conductivity in the weak-relativistic limit, and present the same characteristics, namely a cancellation of the supplementary terms when one considers the total conductivity $\tilde{\sigma}_{ij}^I + \tilde{\sigma}_{ij}^{II}$ (see Appendix B).

²⁶W. H. Butler, Phys. Rev. B **31**, 3260 (1985).

²⁷J. Banhart and H. Ebert, Europhys. Lett. **32**, 517 (1995); J. Banhart, A. Vernes, and H. Ebert, Solid State Commun. **98**, 129 (1996).

²⁸P. Weinberger, P. M. Levy, J. Banhart, L. Szunyogh, and B. Ujfalussy, J. Phys.: Condens. Matter **8**, 7677 (1996).

²⁹D. A. Greenwood, Proc. Phys. Soc. London **71**, 585 (1958).

³⁰A. Fert and A. Hamzic, *The Hall Effect and its Applications*, edited by C. L. Chien and C. R. Westgate (Plenum, New York, 1980), p. 77.

³¹A. Crépieux and P. Bruno, cond-mat/0011426, Phys. Rev. B (to be published).

³²J. Rammer, *Quantum Transport Theory* (Perseus Books, Reading, MA, 1998), p. 322.

³³V. K. Dugaev, A. Crépieux, and P. Bruno, cond-mat/0103182 (unpublished).

³⁴Actually, a third series of diagrams gives a non-zero contribution at order $1/c^0$ to Eq. (29) which is exactly compensated by opposite term in $\tilde{\sigma}_{ij}^{II(0)}$, as discussed in Appendix B.

- ³⁵R. Kubo, Can. J. Phys. **34**, 1274 (1956); J. Phys. Soc. Jpn. **12**, 570 (1957).
- ³⁶J. M. Luttinger, *Mathematical Methods in Solid State and Superfluid Theory*, edited by R. C. Clark and G. H. Derrick (Oliver and Boyd, Edinburgh, 1969), p. 157.
- ³⁷A. Bastin, C. Lewiner, O. Betbeder-Matibet, and P. Nozières, J. Phys. Chem. Solids **32**, 1811 (1971).
- ³⁸P. Štěda, J. Phys. C **15**, L717 (1982).